AD_____

Award Number: DAMD17-02-1-0435

TITLE: The Design, Synthesis, and Biological Evaluation of New Paclitaxel Analogs with the Ability to Evade Efflux by P-Glycoprotein

PRINCIPAL INVESTIGATOR: Brandon J. Turunen
Gunda I. Georg

CONTRACTING ORGANIZATION: The University of Kansas Center for Research, Incorporated
Lawrence, Kansas 66045-7563

REPORT DATE: May 2004

TYPE OF REPORT: Annual Summary

PREPARED FOR: U.S. Army Medical Research and Materiel Command
Fort Detrick, Maryland 21702-5012

REPORT DOCUMENTATION PAGE

Form Approved
OMB No. 074-0188

1. AGENCY USE ONLY (Leave blank)	2. REPORT DATE	3. REPORT TYPE AND DATES COVERED
	May 2004	Annual Summary (1 May 2003 - 30 Apr 2004)

4. TITLE AND SUBTITLE
The Design, Synthesis, and Biological Evaluation of New Paclitaxel Analogs with the Ability to Evade Efflux by P-Glycoprotein

5. FUNDING NUMBERS
DAMD17-02-1-0435

6. AUTHOR(S)
Brandon J. Turunen
Gunda I. Georg

7. PERFORMING ORGANIZATION NAME(S) AND ADDRESS(ES)
The University of Kansas Center for Research, Incorporated
Lawrence, Kansas 66045-7563

E-Mail: bturunen@netscape.net

8. PERFORMING ORGANIZATION REPORT NUMBER

9. SPONSORING / MONITORING AGENCY NAME(S) AND ADDRESS(ES)
U.S. Army Medical Research and Materiel Command
Fort Detrick, Maryland 21702-5012

10. SPONSORING / MONITORING AGENCY REPORT NUMBER

11. SUPPLEMENTARY NOTES
Original contains color plates: All DTIC reproductions will be in black and white.

12a. DISTRIBUTION / AVAILABILITY STATEMENT
Approved for Public Release; Distribution Unlimited

12b. DISTRIBUTION CODE

13. ABSTRACT (Maximum 200 Words)
Paclitaxel, a cytotoxic agent originally isolated fro the bark of the Pacific Yew, has been developed as an effective chemotherapeutic drug, Sadly however, the treatment of cancer with paclitaxel often results in the development of drug resistance. Furthermore, few current chemotherapeutics are able to cross the blood brain barrier leaving victims of brain cancer few viable treatment alternatives.

P-glycoproteins are non-specific transmembrane transporter proteins that are associated with specialized normal tissue barriers, for example the blood brain barrier, and are generally over expressed in tumor cells. These transporter systems recognize a large variety of structurally and functionally diverse chemical entities and are responsible for increasing efflux and decreasing influx of lipophilic substances. This active efflux by P-glycoprotein is believed to be responsible for the development of drug resistance and also the lack of brain uptake. This research focuses on strategies to by-pass P-glycoprotein efflux in order to deliver active, structurally modified paclitaxel analogues to the drug resistant breast cancer cells and/or brain cancer cells.

14. SUBJECT TERMS
Paclitaxel, docetaxel, synthesis, breast cancer, antimetastatic agent

15. NUMBER OF PAGES
29

16. PRICE CODE

17. SECURITY CLASSIFICATION OF REPORT	18. SECURITY CLASSIFICATION OF THIS PAGE	19. SECURITY CLASSIFICATION OF ABSTRACT	20. LIMITATION OF ABSTRACT
Unclassified	Unclassified	Unclassified	Unlimited

Table of Contents

INTRODUCTION

P-glycoproteins are non-specific transmembrane transporters which are present in normal cells and in tumors. They are associated with specialized normal tissue barriers such as the blood brain barrier (BBB), and are generally over expressed in tumor cells. It is believed that active P-glycoprotein efflux of highly lipophilic anti-cancer drugs such as paclitaxel is responsible for the development of drug resistance and also lack of brain uptake.[1,2] The problems in effectively treating drug resistant breast cancer and primary/metastatic brain cancer clearly indicate there is a need for the development of new drug delivery strategies. As the primary focus of this research, endogenous substances are covalently linked to paclitaxel or analogs. Transport carriers exist in the capillary endothelial cells of the blood brain barrier and also in drug resistant breast cancer cells to bring these substances into the cell. By attaching essential hydrophilic molecules such as amino acids, carboxylic acids, amines, and biotin, these paclitaxel analogs may circumvent the P-glycoprotein efflux via active transport into cells/past the BBB. This approach leaves the P-glycoprotein transporters intact and capable of performing their physiological role, potentially a factor for normal tissue survival.[3]

This annual report also serves as a request for modification to our original statement of work. In order to be most productive, the direction of research can, and should, change in accord with results obtained. Below is compiled the results from the last twelve months and will be followed by a revised statement of work proposal. Explanations for stated changes will also be provided therein.

Figure 1. Taxoids

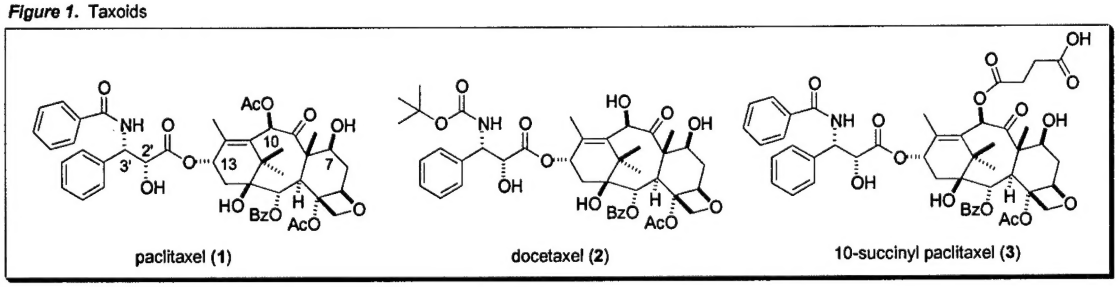

BODY

The synthesis of C7, C10 and C7/C10 analogs of paclitaxel and docetaxel

- Functional Group Analogs of **3**

Scheme 1. C7 and C10 synthetic intermediates

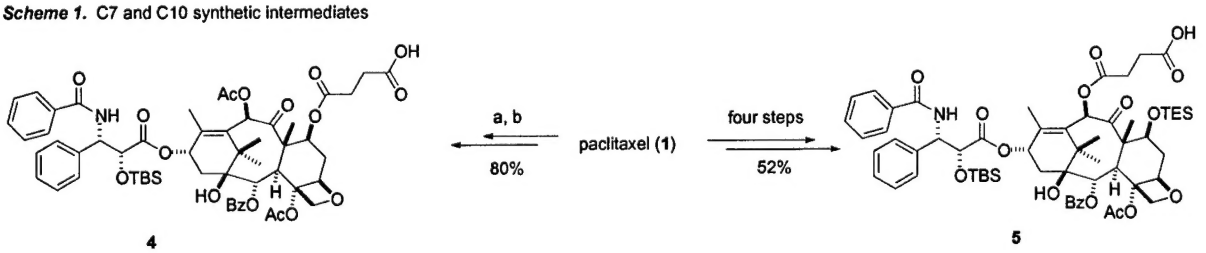

a) TBDMS-Cl, imidizole, CH_2Cl_2; b) succinic anhydride, DMAP, toluene

Prompted by the intriguing biological results of C10 succinyl paclitaxel (**3**), our synthetic efforts have been directed towards the preparation of functional group analogs of it.[4] Initially, as described in the proposal, it was speculated that the succinic acid moiety of **3** was responsible for increased cell

permeation via some sort of active transport shuttle. To further investigate this, additional functional group analogs were prepared. As building blocks for these new compounds, intermediates **4** (previously described) and **5** have been prepared in large quantities in an efficient manner (Scheme 1). From these suitably protected intermediates all compounds in Table 1 have been prepared. Entries 1, 2, and 5 were disclosed last annual report while 2-4 and 6-9 are novel analogs. Standard chemical transformations were employed to prepare the new analogs (see previous annual report, entry 1,2 and 5). To conserve space, this will not be further addressed except to say all reactions proceeded as expected in good to excellent yields.

Table 1. C7 and C10 Succinate Analogs

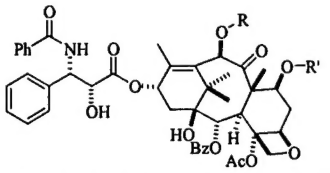

Entry #	R	R'	Entry #	R	R'
TX-67	$COCH_2CH_2CO_2H$	H	5	$COCH_3$	$COCH_2CH_2CO_2H$
1	$COCH_2CH_2CO_2Me$	H	6	$COCH_3$	$COCH_2CH_2CO_2Me$
2	$COCH_2CH_2CONH_2$	H	7	$COCH_3$	$COCH_2CH_2CONH_2$
3	$COCH_2CH_2CONHMe$	H	8	$COCH_3$	$COCH_2CH_2CONHMe$
4	$COCH_2CH_2CONMe_2$	H	9	$COCH_3$	$COCH_2CH_2CONMe_2$

- C7/C10 Paclitaxel and Docetaxel succinate derivatives

To further expand upon structure-activity relationship (SAR) data on our lead compound (**3**), terminal carboxylic acid units with varied length and position have been attached to paclitaxel and docetaxel. (Table 2). The preparation of the docetaxel utilized to prepare entries 4-6 (Table 2) was described in the previous annual report. Succinic as well as glutaric acids have been placed on C7, C10 and both C7/C10 as proposed.

Table 2. Various Acid Analogs

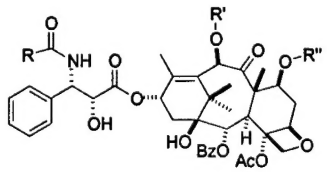

Paclitaxel R=Ph (**1**)
Docetaxel R=*t*-butoxy (**2**)

Entry #	R	R'	R"
TX-67	Ph	$CO(CH_2)_2CO_2H$	H
1	Ph	$CO(CH_2)_3CO_2H$	H
2	Ph	$COCH_3$	$CO(CH_2)_2CO_2H$
3	Ph	$COCH_3$	$CO(CH_2)_3CO_2H$
4	*t*-butoxy	$CO(CH_2)_2CO_2H$	H
5	*t*-butoxy	$CO(CH_2)_3CO_2H$	H
6	*t*-butoxy	$CO(CH_2)_2CO_2H$	$CO(CH_2)_2CO_2H$

- Nutrient Vectors: Biotin and Phenylalanine

As described previously, the proposed C7 biotinolated analog **6** (Scheme 2) has been prepared. It was planned to utilize intermediate **5** and ethylene diamine biotin to prepare the C10 biotinylated analog. By performing the coupling further from the congestion of the baccatin core, it was anticipated

Scheme 2. Biotin Paclitaxel

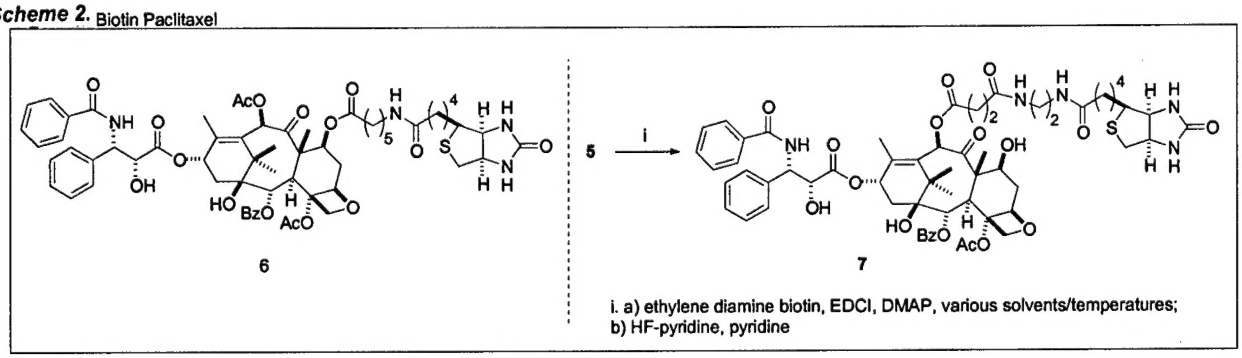

i. a) ethylene diamine biotin, EDCI, DMAP, various solvents/temperatures;
b) HF-pyridine, pyridine

that a more productive union be accomplished lending to formation of **7** following deprotection. Experimentation demonstrated that the coupling of **5** with the ethylene diamine biotin was not as facile as anticipated. Initial conditions entailed those which we commonly employ for these types of couplings (room temp, CH_2Cl_2, EDCI, NMM) however only starting material was recovered under these conditions. After screening a variety of progressively more vigorous conditions it was found that refluxing in DMF with the addition of excess DMAP, EDCI, and the biotin analog allowed for said transformation. The silyl protecting groups were then removed to provide compound **7**. Due to the extreme polarity of this compound, isolating material of high enough purity for biological testing has been difficult. More of this compound is currently being prepared and attempts at recrystallization will be employed.

The protected variant of our desired C10 phenylalanine analog (**8**) was prepared and disclosed last annual report. In a similar fashion, from intermediate **4**, the protected variant of the corresponding C7 analog has been prepared using conditions described in Scheme 3. Unfortunately, all attempts to remove the benzyl and benzoyl protecting groups form the amino acid moiety have been unsuccessful

Scheme 3. Phenylalanine Paclitaxel

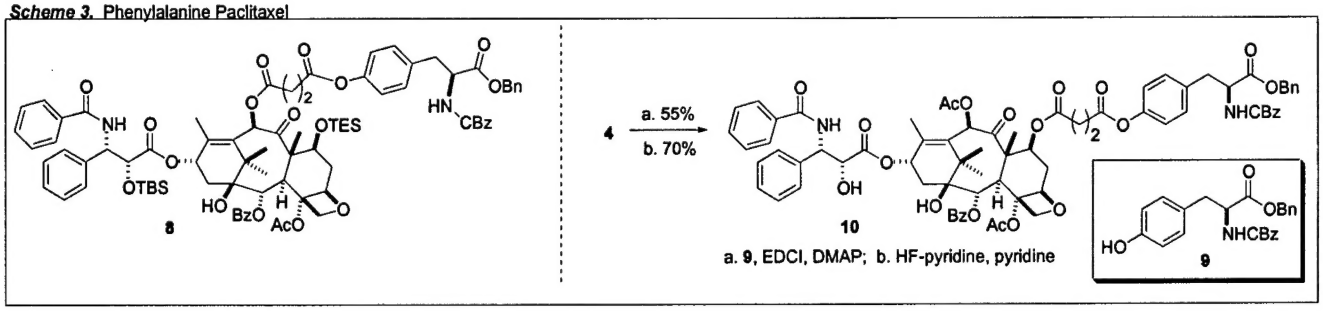

and only starting material has been recovered from these reactions. To remedy this problem, we propose employing amino acid analog **10**. We have prepared this compound in three steps from commercially available 4-Nitro-L-phenylalanine (Scheme 4).[5] Although the Boc protecting group will need to be removed, this two step procedure should allow for the exposure of the desired amino acid. Additionally, this modification removes the biologically labile ester linkage of compounds **8** and **10** and replaces it with a more robust amide linkage.

Scheme 4. Modified Route to Phenylalanine Analogs

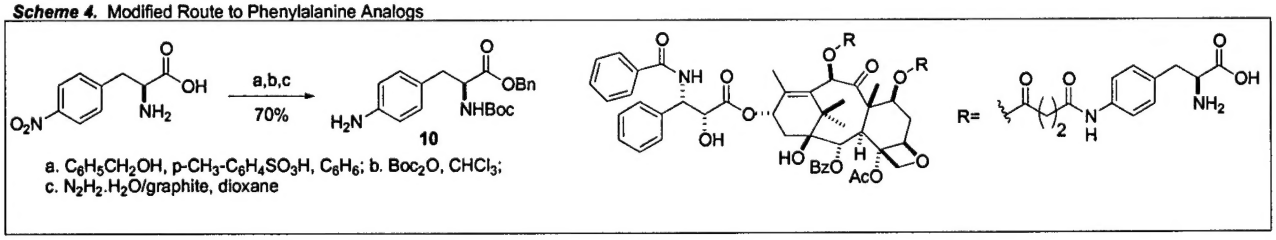

Biological Evaluation

Tubulin Assembly, Cytotoxicity

Tubulin assembly and cytotoxicity data for all compounds except table 2, entry 3 (T2, E3). This analog is pending analysis (PA). Based upon the functional group analogs generated (T1, E1-E9), it appears that *removal of the carboxylic acid functionality does not have an adverse effect on cytotoxicity toward breast cancer cell lines or drug resistant breast cancer cell lines*. In fact, many of the amides and esters performed better than the corresponding acid analog.

Increasing the length and placement of the acid moiety seemed to have a detrimental effect as all compounds in table 2 (T2, E1 and E3-E6) lost potency against MCF-7 cell lines. None of these analogs showed an increase in activity against the drug resistant (Pgp-overexpressing) cell lines. Even the docetaxel analogs (T2, E4-E6) did not demonstrate reasonable activity. The biotin analog **6** also lost efficacy toward MCF-7 and MCF7-ADR.

The most promising compounds, the functional group analogs T1 E1-E9, were able to maintain similar or superior activity comparative to our lead compound as well as paclitaxel. The compounds were therefore further evaluated for interactions with P-glycoprotein.

Table 3. ED_{50}/ED_{50}(paclitaxel)

Analog	Tubulin Assembly[a]	MCF-7[b]	MCF7-ADR[c]
Taxol	1.0	1.0	1.0
TX-67	1.7	>13	>1.3
T1, E1	1.0	0.76	0.43
T1, E2	0.4	4.0	6.0
T1, E3	0.8	7.9	6.0
T1, E4	1.6	2.1	2.7
T1, E5	3.8	1300	5.8
T1, E6	1.2	1.0	0.5
T1, E7	0.6	3.2	0.66
T1, E8	0.8	2.2	1.0
T1, E9	1.1	10.8	0.82
T2, E1	1.8	>15	>2.9
T2, E2 = T1, E5			
T2, E3	PA	PA	PA
T2, E4	2.3	>15	>2.9
T2, E5	1.5	>15	2.6
T2, E6	3.8	>15	>2.9
6	0.9	>15	>15

a. ED_{50} is the concentration which causes polymerization of 50% of the tubulin present in 15 min at 37°C. ED_{50} of paclitaxel: 0.4 to 0.6 uM. b: ED_{50} refers to the concentration which produces 50% of proliferation of MCF-7 cells after 72h incubation. ED_{50} of paclitaxel: 2 to 4 nM. c. ED_{50} refers to the concentration which produces 50% of proliferation of MCF7-ADR cells after 72h incubtion. ED_{50} of paclitaxel: ~2500 nM

Rhodamine 123 uptake assay

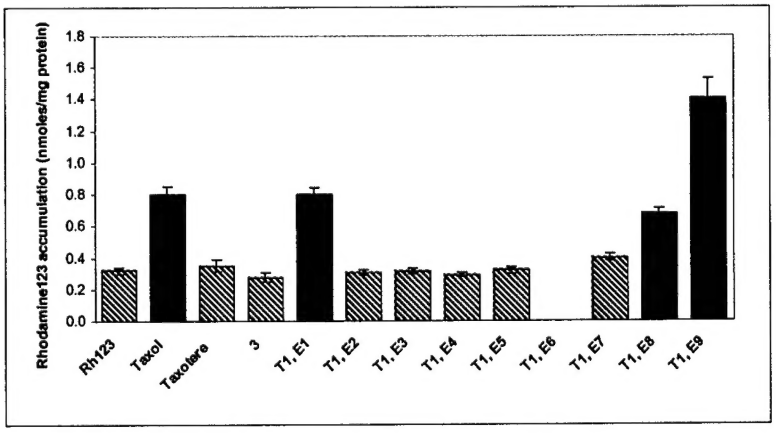

The adjacent chart illustrates interactions of tested compounds with P-glycoprotein present in bovine brain microvessel endothelial cells (BMEC). Please see the original proposal for a description of the assay. The compounds indicated in red (paclitaxel, T1 E1, T1 E8, and T1 E9) interact with P-gp and are therefore substrates. Compound T1 E6 is pending analysis. All C10 succinate analogs (3, T1 E2-E4), excluding the methyl ester (T1 E1), did not interact with P-gp. The C7 succinic acid as well as the primary amide did not interact with P-gp yet the substituted amides do interact with P-gp.

Key Research Accomplishments

- Preparation of C7 and C10 carboxylic acid analogs
- Preparation of C7 and C10 functional group analogs
- Preparation of C7 and C10 biotin analog
- Preparation of protected variant of C7 and C10 phenylalanine analog
- Asymmetric synthesis of docetaxel side chain as well as docetaxel
- Synthesis of 3'N analogs
- Tubulin assembly and cytotoxicity data obtained for described analogs
- Rhodamine 123 uptake studies completed for identified analogs

Reportable Outcomes

- *Journal of Neurochemistry*, 2003, **84**, 347-362 (see attached)
- *Journal of Molecular Neuroscience*, 2003, **3**, 339-344 (see attached)
- M. S. Medicinal Chemistry, University of Kansas, 2003
- Completion of all requirements for Ph. D. in Medicinal Chemistry, expected May 2005
- Secured post-doctoral researcher position in the laboratory of Barry M. Trost, Department of Chemistry, Stanford University (May 2005)

Conclusions

In the first two years of funding many novel analogs have been generated and useful biological information has been gained. The compounds have shown much promise in preliminary in vitro and in vivo assays in regards to BBB penetration and two papers have been generated as a result. The carboxylic acid moiety is not required for evasion of P-gp. Contrary to our original hypothesis, compounds which do not interact with brain P-gp appear to still be P-gp substrates in drug resistant breast cancer cell lines. This may indicate different subtypes of P-gp present or could implicate other resistance mechanisms in breast cancer cell lines. Based upon these results a modest redirection in research is warranted. A revised statement of work will be submitted supporting this.

References

(1) Schinkel, A. H.; Smit, J. J. M.; van Tellingen, O.; Beijnen, J. H.; Wagenaar, E.; van Deemter, L.; Mol, C. A. A. M.; van der Valk, M. A.; Robanus-Maandag, E. C.; te Riele, H. P. J.; Berns, A. J. M.; Borst, P. Disruption of the Mouse *mdr1a* P-Glycoprotein Gene Leads to a Deficiency in the Blood-Brain Barrier and to Increased Sensitivity to Drugs. *Cell* **1994**, *77*, 491-502.

(2) Schinkel, A. H.; Wagenaar, E.; Mol, C. A. A. M.; van Deemter, L. P-Glycoprotein in the Blood-Brain Barrier of Mice Influences the Brain Penetration and Pharmacological Activity of Many Drugs. *J. Clin. Invest.* **1996**, *97*, 2517-2524.

(3) Burton, P. S.; Conradi, R. A.; Hilgers, A. R.; Ho, N. F. H. Evidence for a Polarized Efflux System for Peptides in the Apical Membrane of Caco-2 Cells. *Biochem. Biophys. Res. Commun.* **1993**, *190*, 760-766.

(4) Li, G.; Faibushevich, A.; Turunen, B. J.; Yoon, S. O.; Georg, G. I.; Michaelis, M. L.; Dobrowski, R. T. Stabilization of the cyclin-dependant kinase 5 activator, p35, by paclitaxel decreases β-amyloid toxicity in cortical neurons. *Journal of Neurochemistry*, **2003**, *84*, 347-362.

(5) Larden, D. W.; Cheung, H. T. A. Synthesis of α-Aminoacyl Derivatives of Melphalan for Use in Antibody Directed Enzyme Pro-drug Therapy. *Tetrahedron*, **1999**, *55*, 3265-3267.

Journal of Neurochemistry, 2003, **84**, 347–362

Stabilization of the cyclin-dependent kinase 5 activator, p35, by paclitaxel decreases β-amyloid toxicity in cortical neurons

Guibin Li,* Alexander Faibushevich,* Brandon J. Turunen,‡ Sung Ok Yoon,† Gunda Georg,‡ Mary L. Michaelis* and Rick T. Dobrowsky*

**Department of Pharmacology and Toxicology, ‡Department of Medicinal Chemistry, University of Kansas, Lawrence, Kansas*
†Neurobiotech Center and Department of Neuroscience, Ohio State University, Columbus, Ohio, USA

Abstract

One hallmark of Alzheimer's disease (AD) is the formation of neurofibrillary tangles, aggregated paired helical filaments composed of hyperphosphorylated tau. Amyloid-β (Aβ) induces tau hyperphosphorylation, decreases microtubule (MT) stability and induces neuronal death. MT stabilizing agents have been proposed as potential therapeutics that may minimize Aβ toxicity and here we report that paclitaxel (taxol) prevents cell death induced by Aβ peptides, inhibits Aβ-induced activation of cyclin-dependent kinase 5 (cdk5) and decreases tau hyperphosphorylation. Taxol did not inhibit cdk5 directly but significantly blocked Aβ-induced calpain activation and decreased formation of the cdk5 activator, p25, from p35. Taxol specifically inhibited the Aβ-induced activation of the cytosolic cdk5-p25 complex, but not the membrane-associated cdk5-p35 complex. MT-stabilization was necessary for neuroprotection and inhibition of cdk5 but was not sufficient to prevent cell death induced by overexpression of p25. As taxol is not permeable to the blood–brain barrier, we assessed the potential of taxanes to attenuate Aβ toxicity in adult animals using a succinylated taxol analog (TX67) permeable to the blood–brain barrier. TX67, but not taxol, attenuated the magnitude of both basal and Aβ-induced cdk5 activation in acutely dissociated cortical cultures prepared from drug treated adult mice. These results suggest that MT-stabilizing agents may provide a therapeutic approach to decrease Aβ toxicity and neurofibrillary pathology in AD and other tauopathies.

Keywords: amyloid-β, calpain, cyclin-dependent kinase 5, microtubules, paclitaxel, tau.
J. Neurochem. (2003) **84**, 347–362.

Alzheimer's disease (AD) is characterized by the loss of specific groups of neurons and the presence of two brain lesions, amyloid plaques and neurofibrillary tangles (NFTs) (Lee *et al.* 2001; Selkoe 2001b). NFTs are composed of intracellular aggregates of highly insoluble paired helical filaments (PHFs) made up of fibrils of the MT-associated protein tau (Goedert 1997). Although the relationship between these two principal lesions is unclear, the discovery that multiple *tau* gene mutations occur in frontotemporal dementia and parkinsonism linked to chromosome 17 (FTDP-17) has provided strong evidence that tau abnormalities are sufficient to promote neurodegeneration (Scheuner *et al.* 1996; Goedert *et al.* 1998; Spillantini *et al.* 1998)., Abnormal phosphorylation of tau by Aβ peptides promotes the loss of its microtubule (MT) stabilizing ability (Busciglio *et al.* 1995) and contributes to neurite degeneration and the formation of PHFs (Lee *et al.* 2001). These observations led to the hypothesis that MT-stabilizing agents, such as paclitaxel (taxol), might help overcome the inadequate binding of hyperphosphorylated tau to MTs and slow the progression of neurofibrillary pathology and cell death (Lee *et al.* 1994). We have reported previously that taxol can protect primary cortical neurons from Aβ-induced cell death (Michaelis *et al.* 1998). However, whether the neuroprotective action of taxol resulted solely from increased

Received August 13, 2002; revised manuscript received October 8, 2002; accepted October 11, 2002.

Address correspondence and reprint requests to Rick T. Dobrowsky, Department of Pharmacology and Toxicology, University of Kansas, 5064 Malott Hall, 1251 Wescoe Hall Dr, Lawrence, KS 66045, USA.
E-mail: dobrowsky@ku.edu

Abbreviations used: Aβ, amyloid-beta; AD, Alzheimer's disease; cdk5, cyclin-dependent kinase 5; CNS, central nervous system; DAB, 10-deacetylbaccatin III; JNK, c-*jun* N-terminal kinase; MTs, microtubules; NFTs, neurofibrillary tangles; PHFs, paried helical filaments; TX67, 10-succinyl paclitaxel.

MT-stabilization or had contributions from other effects, such as regulating tau phosphorylation, was unclear. The cascade of events that lead to tau hyperphosphorylation may be a critical step in the pathogenesis of tauopathies (Goedert *et al.* 1998). Although tau is phosphorylated by numerous kinases *in vivo* (Billingsley and Kincaid 1997), recent attention has focused upon the role of cdk5 as an important tau kinase whose activity is enhanced in response to Aβ in cultured neurons (Alvarez *et al.* 1999, 2001) and in AD brain (Lee *et al.* 1999; Patrick *et al.* 1999). Cdk5 is a 33-kDa serine/threonine kinase that is active primarily in neurons (Ino *et al.* 1994) and can associate with MTs indirectly (Sobue *et al.* 2000). Cdk5 activity is regulated through association with the specific cyclin-related activator molecules, p35, p39, p25 and p29 (Dhavan *et al.* 2001). The calpain-directed proteolysis of p35/p39 (Kusakawa *et al.* 2000; Lee *et al.* 2000; Nath *et al.* 2000; Patzke and Tsai 2002a) releases p25/p29 from an N-terminal membrane tether and may delocalize cdk5/p25 (cdk5/p29) complexes from the plasma membrane and decrease phosphorylation of physiologic membrane substrates (Niethammer *et al.* 2000; Zukerberg *et al.* 2000). p35 has a short cellular half-life (Patrick *et al.* 1998, 1999) and its increased degradation can lead to cytoplasmic accumulation of cdk5/p25 complexes (Dhavan *et al.* 2001). As overexpression of cdk5/p25 in cells (Patrick *et al.* 1999) or transgenic mice (Ahlijanian *et al.* 2000) enhances tau phosphorylation, the ability of cdk5/p25 but not cdk5/p35 to serve as a tau kinase has lead to the concept that tau is a pathological substrate for cdk5 (Dhavan *et al.* 2001). Thus, treatments that affect the turnover and/or production of p35 should indirectly impact on cdk5 activity. In this report, we demonstrate that taxol inhibits an Aβ-induced pathway that links increased calpain activity to enhanced p25 production, cdk5 activation and tau phosphorylation. Although MT-stabilization by taxol was necessary for neuroprotection and inhibition of cdk5 activity, it was not sufficient to protect neurons from constitutive cdk5 activation following overexpression of p25 in primary cortical neurons. As the therapeutic potential of taxol in AD is limited by its bioavailability to the brain, we show that administration to adult mice of a taxol analog permeant to the blood–brain barrier inhibits Aβ-induced cdk5 activation. Collectively, our data suggest that MT-stabilization is tightly linked to the regulation of tau phosphorylation and that MT-stabilizing drugs may be potential therapeutic agents to slow the development of neurofibrillary pathologies.

Experimental procedures

Materials

Polyclonal antibodies directed against cdk5 (C-8), the C-terminus of p35 (C-19) and the N-terminus of p35 (N-20) were obtained from Santa Cruz Biotechnology (Santa Cruz, CA, USA). AT-8 antibody was purchased from Endogen and the Tau-5 and PHF-1 antibodies were provided by Dr Peter Davies (Albert Einstein College of Medicine). The pAdTrack-CMV (cytomegalovirus) shuttle vector and pAdEASY-1 adenoviral backbone vector were generous gifts from Dr T. C. He (Johns Hopkins University Medical School). Dr L-H. Tsai (Harvard Medical School) kindly provided the p35 cDNA construct. Taxol was purchased from Dabur India, Ltd. and the succinylated taxol analog (TX67) was prepared by parallel solution phase synthesis (Liu *et al.* 2002). Histone H1, bovine brain tau, N-succinyl-leu-tyr-7-amido-4-methylcoumarin, and $A\beta_{1-42}$ peptides were purchased from Sigma/Aldrich Chemicals (St Louis, MO, USA). $A\beta_{25-35}$ was synthesized by the Biochemical Research Services Laboratory at the University of Kansas. [γ-^{32}P]ATP was from DuPont–NEN, Boston, MA, USA.

Cell culture and drug administration

Primary cortical neurons were prepared from embryonic day 18 Sprague-Dawley rat pups as described previously (Michaelis *et al.* 1994). Following trituration, the cells were resuspended in Dulbecco's modified Eagle's medium/F12 (DMEM/F12) containing 15 mM $KHCO_3$, 10% fetal calf serum and plated onto 35 or 60 mm poly D-lysine-coated dishes at a density of 6.5×10^5 or 2×10^6 cells/dish for viability and biochemical assays, respectively. Twenty-four hours after plating, the cells were washed and placed in defined medium (DMEM/F12, 0.1 g/L transferrin-APO form, 5 mg/L insulin, 0.1 mM putrescine, 10 nM progesterone, 30 nM sodium selenite, and 1 mM sodium pyruvate) for the duration of the experiment. After 4 days *in vitro*, the cells were treated with 10 μM Aβ peptides in the absence or presence of 100 nM taxol. Taxol was stored as a 1 mM stock solution in dimethyl sulfoxide (DMSO) and diluted to 25 μM in H_2O prior to the experiment. The final concentration of DMSO in all cultures was 0.01%.

TX67 is a substituted taxol analog that replaces the C-10 acetyl group of taxol with succinic acid (Liu *et al.* 2002). Adult mice received intraperitoneal injections (0.1 mL) of 8 mg/kg TX67 every 2 days over 16 days. TX67 was dissolved in a (1 : 1) solution of ethanol/Cremephor EL (polyethoxylated castor oil that is used clinically for taxol injections) and diluted 1 : 6 with 133 mM sterile saline immediately prior to injection. Animals receiving taxol were treated similarly. The dosing schedule appeared to have little effect on the general health of the animals, as all gained weight and displayed no obvious behavioral or physical anomalies. All animal procedures were performed in accordance with protocols approved by the Institutional Animal Care and Use Committee and in compliance with standards and regulations for care and use of laboratory rodents set by the National Institutes of Health.

Cultures of acutely dissociated neurons from the control and drug-treated animals were prepared after killing the animals with CO_2. The brains were rapidly excised and placed in ice-cold isotonic buffer (5.0 mM HEPES, pH 7.4, 132 mM NaCl, 5.36 mM KCl, 0.21 mM Na_2HPO_4, 0.22 mM KH_2PO_4, 2.77 mM glucose and 58.4 mM sucrose). The cerebral cortices were dissected, the grey matter minced into small pieces and the tissue incubated with 0.25% trypsin in calcium and magnesium free Hank's solution for 1 h at 37°C. The tissue fragments were triturated to disperse the cells and placed into 20 mL of DMEM/F12 medium containing 10% fetal calf serum and 15 mM $KHCO_3$. The cell suspension was filtered through a sterile 41 μm nylon mesh filter to remove large clumps, the cells

collected by centrifugation and resuspended in pre-warmed DMEM/F12 medium containing 10% fetal calf serum. The cells were treated immediately with 20 μM $A\beta_{25-35}$ for 24 h and both adherent and non-adherent cells were harvested, resuspended in lysis buffer and *ex vivo* cdk5 activity assessed as described below.

Immunoprecipitation of Cdk5 and *in vitro* kinase assay

Cells were harvested in lysis buffer (20 mM Tris-HCl pH 7.4, 140 mM NaCl, 1 mM PMSF, 1 mM Na_3NO_4, 10 mM NaF, 0.1% Nonidet-40, 1 mM EDTA, 1 × complete protease inhibitors (Roche Diagnostics, Indianapolis, IN, USA) and 26 μM *N*-acetyl-leu-leu-norleucinal, ALLN) and cell debris was removed by centrifugation at 10 000 *g* for 10 min at 4°C. Protein concentration was determined using the Bio-Rad dye and bovine serum albumin as the standard. Protein (200 μg) was incubated with 2 μg of Cdk5 antibody (C-8) or p35 antibodies (N-20 or C-19) for 2 h at 4°C. Protein A-Sepharose beads (40 μL of a 50% slurry) were added to the samples and immune complexes were formed by incubation for 1 h at 4°C. The beads were sedimented by centrifugation, washed two times with lysis buffer and one time with kinase buffer (50 mM Tris-HCl, pH, 7.4, 80 mM β-glycero-phosphate, 20 mM EGTA, 15 mM $MgCl_2$, and 1 mM dithiothreitol). The beads were resuspended in 30 μL of kinase buffer containing 50 μM ATP, 1.25 μCi of [γ-^{32}P]ATP, and 1 μg of histone H1 or purified tau protein. The samples were incubated at 24°C for 30 min (histone H1) or 37°C for 30 min (tau) and the reaction was stopped by adding 10 μL of 4 × sodium dodecyl sulfate–polyacrylamide gel electrophoresis (SDS–PAGE) loading buffer. Proteins were separated by SDS–PAGE and the radioactive bands were quantified using a phosphoimager.

In some experiments, cdk5 was immunoprecipitated from cytosolic and particulate fractions. Neurons were treated with Aβ in the absence and presence of taxol and scraped into detergent-free lysis buffer to avoid solubilizing membrane bound cdk5/p35. The cells were sonicated and debris was removed by centrifugation at 10 000 *g* for 5 min. An aliquot of the whole cell lysate was removed (100 μg) and 100 μg was centrifuged at 100 000 *g* for 1 h at 4°C in a table top Optima-Max ultracentrifuge. The supernatant (cytosol) was transferred to a fresh tube and Nonidet-40 was added to a final concentration of 0.1%. The pellet (membrane) was washed and then solubilized in lysis buffer containing 0.1% Nonidet-40. Cdk5 was immunoprecipitated from the cytosolic and membrane fractions with 2 μg of the C-19 p35 antibody and kinase activity assessed as described above.

Cell viability measurements

$A\beta_{25-35}$ (1.3 mg/mL) and $A\beta_{1-42}$ (4.5 mg/mL) were prepared by resuspending the peptides in H_2O followed by dilution with 10 mM Tris-HCl, pH 7.4, to 1 mM. The peptides were then aged at 37°C for 24 h to induce aggregation. Cell viability was determined using the live/dead assay as described previously (Michaelis *et al.* 1998). The cells were stained with 10 μM propidium iodide (PI) and 150 nM calcein-acetoxymethylester (calcein-AM, Molecular Probes, Eugene, OR, USA) for 30 min at 37°C and imaged by fluorescence microscopy. Six images were captured from each dish on marked fields with a CCD camera and all the cells in each field were counted to determine total cell number. Calcein-AM labels the viable cells (green) and PI stains the dead cells (red). Cell viability was calculated as a percentage of viable cells to total cell number.

Protein half-life assay

Neurons were treated with vehicle or taxol for 4 days followed by the addition of 30 μg/mL cycloheximide for 0–480 mins (Patrick *et al.* 1998). At the indicated time, the cells were scraped into lysis buffer, cell debris was removed by centrifugation at 10 000 *g* for 10 min at 4°C and an equal amount of protein from each time point was subjected to SDS–PAGE. In assessing the effect of Aβ and taxol treatment on p35/p25 levels, complete protease inhibitors and 26 μM ALLN were always added to the lysis buffer immediately before harvesting and the samples were processed directly for SDS–PAGE without freezing and thawing of the lysates. The proteins were transferred to nitrocellulose and p35/p25 detected by immunoblot analysis using a C-terminal antibody. The blot was stripped and re-probed for the presence of tau (tau-5 antibody) and cdk5. The amount of p35 expression at each time point was quantified by densitometry and expressed as per cent remaining relative to that present at time 0.

Calpain activity assay

Neurons were harvested after 4 days of treatment in calpain lysis buffer (20 mM Tris pH 7.4, 140 mM NaCl, 0.1% Nonidet-40) and cell debris was removed by centrifugation as described above. Protein (30 μg) from each sample was loaded in quadruplicate to a 96-well plate and the reaction initiated with 130 μM substrate without the addition of exogenous calcium. The substrate for this assay, *N*-succinyl-leu-tyr-7-amido-4-methylcoumarin, is a non-fluorescent peptide which strongly fluoresces after cleavage by calpain (Xie and Johnson 1997). The increase in fluorescence intensity was recorded at 30°C for 3 h in a Bio-Tek FL600 microplate fluorometer and normalized to total protein. In some assays, 100 nM taxol was added directly to the reaction mix containing 0.4 units of purified calpain 1 (Calbiochem, San Diego, CA, USA) and 5 mM Ca^{2+} in lysis buffer.

Generation of p25 recombinant adenovirus

p35-pcDNA3 served as a template for amplifying p25 by PCR. The forward primer (5′-GTCGACGGTACCATGGCCCAGCCCC-CACCG-3′) incorporated a *Kpn*I site and an ATG start codon upstream of the N-terminal alanine for p25 (amino acid 98 of p35) (Tsai *et al.* 1994). The reverse primer (5′-CTCGAGTTACCGA TCCAGGCCTAG-3′) was engineered with a *Xho*I site. The amplified PCR product was subcloned directly into TOPO2.1 (Invitrogen, Carslbad, CA, USA) and sequenced in both directions for errors. The p25-TOPO2.1 cDNA was digested with *Kpn*I and *Xho*I, the approximate 0.6-kb p25 fragment was gel purified and subcloned into the pAdTrack-CMV shuttle vector (He *et al.* 1998). p25-AdTrack-CMV was linearized with *Pme*I and electroporated into $RecA^+$ bacteria (BJ5183) with 1 μg of pAdEASY-1 as described (He *et al.* 1998). Bacterial clones containing recombinant adenoviral DNA were verified by restriction mapping and recombinant viruses were generated by transfection of HEK293 cells. Virus was amplified by four rounds of infection and purified from 20 × 15 cm plates of HEK293 cells using two rounds of centrifugation through CsCl gradients. The residual CsCl was removed by dialysis against 10 mM Tris-HCl, pH 8.0, 100 mM NaCl, 0.1% bovine serum albumin, 20% glycerol in a Slide-a-Lyzer cassette. Recombinant adenoviruses were titered based upon number of green fluorescent foci in an agar-overlay assay as described (He *et al.* 1998). Cortical neurons were infected with blank or

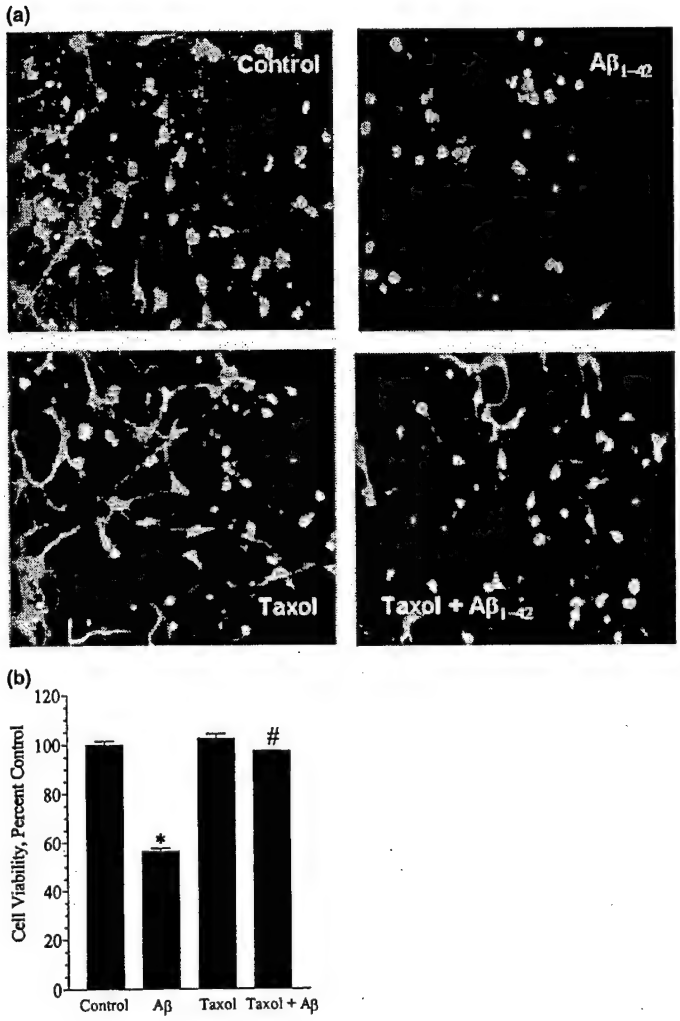

Fig. 1 Cell death induced by $A\beta_{1-42}$ is prevented by taxol pre-treatment. (a) Neurons were treated with buffer, 100 nM taxol or 10 μM $A\beta_{1-42}$ in the absence or presence of taxol for 4 days. The cells were stained with calcein-AM and propidium iodide, photographed and cell viability determined. (b) The results from the quantitative analysis of neuronal viability from three experiments. *, $p < 0.001$ compared with control; #, $p < 0.001$ compared with Aβ only. At least 200 cells per treatment were counted in each experiment.

p25-recombinant adenoviruses at 100–400 pfu/cell. The infection efficiency as monitored by cells expressing the green fluorescent protein ranged from 40 to 50%.

Statistical analysis

All results are presented as means ± SEM and statistically relevant differences between treatments within a data set were determined using a one-way ANOVA with subsequent post hoc analysis using Tukey's-test.

Results

Taxol protects against cell death induced by Aβ peptides

Primary neuronal cell cultures derived from the brains of embryonic rat pups (Michaelis *et al.* 1994) were used to demonstrate the protective effect of taxol against Aβ-induced toxicity. Taxol pre-treated cells were minimally distinguishable from control cells, indicating that the MT-stabilizing properties of the drug did not affect neuronal morphology (Fig. 1a). Our previous studies solely used the $A\beta_{25-35}$ peptide to assess the effect of taxol on cell death (Michaelis *et al.* 1998), but this Aβ peptide fragment is not produced in AD. Therefore, we assessed the effect of taxol against neuronal toxicity induced by $A\beta_{1-42}$, the physiologically relevant Aβ peptide that accumulates in AD (Selkoe 2001a). Whereas cells treated with $A\beta_{1-42}$ were pyknotic with fragmented and degenerating neurites, taxol preserved neurite morphology and overall appearance in the presence of $A\beta_{1-42}$ (Fig. 1a). Further, quantitation of cell survival indicated that 100 nM taxol afforded significant protection against cell death induced by 10 μM $A\beta_{1-42}$ (Fig. 1b). As taxol rescues neurons against cell death induced by $A\beta_{1-42}$ with results qualitatively similar to $A\beta_{25-35}$, most remaining studies used this shorter Aβ peptide.

Table 1 TX67 but not 10-deacetylbaccatin III protects cortical neurons against Aβ toxicity

	Cell viability	Per cent control
	Minus Aβ	Plus Aβ
Vehicle	100	57.6 ± 4.6[a]
10-deacetylbaccatin III	91.3 ± 1.2	60.5 ± 3.2[a]
10-succinyl taxol (TX-67)	93.7 ± 3.4	85.3 ± 2.9[b]

Neurons were pre-treated for 2 h with 100 nM of the indicated drug and the cells were stimulated with 10 μM $A\beta_{25-35}$. After 4 days, cell viability was determined with the live/dead assay. [a]$p < 0.001$ compared with vehicle minus Aβ, [b]$p < 0.001$ compared with vehicle plus Aβ.

To assess whether the neuroprotective effects of taxol required MT-stabilization, cells were treated with 10-deactylbaccatin III, a taxol precursor that is ineffective at stabilizing MTs (Wang *et al.* 1998). 10-Deactylbaccatin III provided no significant protection against $A\beta_{25-35}$ toxicity (Table 1) which strongly supports that the MT-stabilizing properties of taxol are indeed necessary for neuroprotection. As neurons undergoing Aβ-induced degeneration exhibit increased phosphorylation of the MT-interacting protein tau which leads to MT destabilization (Busciglio *et al.* 1995), taxol may help maintain MT stability and consequently regulate the interaction of tau with Aβ-activated tau kinases. Therefore, we addressed the possibility that taxol may decrease Aβ toxicity by stabilizing MTs and interfering with mechanisms regulating Aβ-induced tau hyperphosphorylation.

Taxol inhibits Aβ-induced tau phosphorylation

To assess the *in vivo* effect of $A\beta_{25-35}$ and taxol treatment on tau phosphorylation in primary neurons, we used the AT-8, PHF-1 and Tau-5 antibodies. AT-8 recognizes an epitope phosphorylated at Ser202 and Thr205 while PHF-1 recognizes tau phosphorylated on Ser396 and Ser404 (Busciglio *et al.* 1995). The Tau-5 antibody recognizes total tau levels independent of phosphorylation state.

Neurons were pre-treated with 100 nM taxol for 2 h and challenged with 10 μM $A\beta_{25-35}$. After an additional 4 days, cell lysates were prepared and the proteins present in a post-nuclear supernatant fraction were resolved by SDS–PAGE. After transferring the proteins to nitrocellulose, tau phosphorylation and total tau levels were determined by immunoblot analysis. $A\beta_{25-35}$ significantly increased the amount of hyperphosphorylated tau detected by both the AT-8 and PHF-1 antibodies (Fig. 2a). Increased hyperphosphorylation was completely prevented by taxol which had no effect on total tau levels as determined using the Tau-5 antibody. Moreover, the Tau-5 antibody also recognizes phosphorylated tau species as indicated by the presence of a mobility shift in the tau band from cells treated with $A\beta_{25-35}$. This species of tau was also abolished in the taxol-treated cells. The expression of cdk5 also remained the same in all the treatments and provides an additional control for protein loading. Densitometric quantitation of the PHF-1 immunoreactive bands from several experiments indicated that taxol significantly decreased both basal and Aβ-induced tau phosphorylation (Fig. 2b).

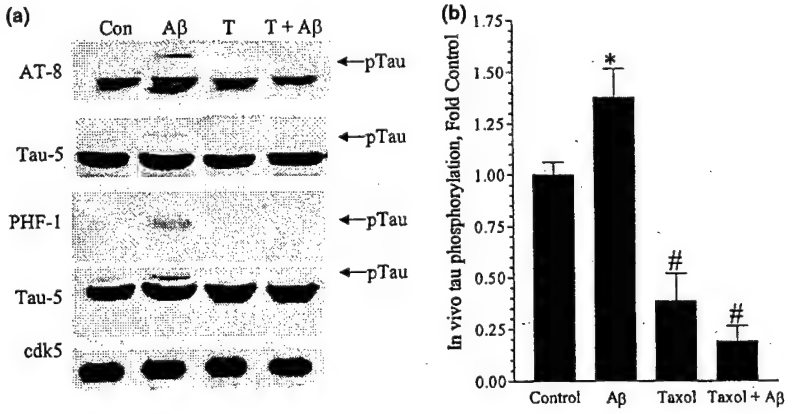

Fig. 2 Taxol blocks Aβ-induced tau hyperphosphorylation. (a) Neurons were exposed to buffer (Con), 100 nM taxol (T) or 10 μM $A\beta_{25-35}$ in the absence (Aβ) or presence of taxol (T + Aβ) for 4 days. Whole cell lysates were prepared and total protein was separated by SDS–PAGE (20 μg/lane). After transfer to nitrocellulose, the membrane was probed for phosphorylated tau (AT-8 or PHF-1 antibodies), stripped and re-probed for total tau using the Tau-5 antibody. Phosphorylated tau (pTau) is indicated by the arrows. Bottom panel shows the expression level of cdk5 from the same samples. (b) Tau phosphorylation detected with the PHF-1 antibody was quantitated by densitometry from five experiments. *, $p < 0.05$ compared with control; #, $p < 0.001$ compared with $A\beta_{25-35}$ only.

Taxol blocks Aβ-induced activation of cdk5/p25 complexes

Tau is phosphorylated by numerous kinases *in vivo* including glycogen synthase kinase 3β, MT-affinity regulated kinases, protein kinase A and cdk5 (Billingsley and Kincaid 1997; Lee *et al.* 2001; Maccioni *et al.* 2001). $A\beta_{25-35}$ slightly stimulated glycogen synthase kinase 3β (~1.2-fold) under our culture conditions and taxol inhibited this activation (data not shown). However, $A\beta_{25-35}$ more robustly and reproducibly activated cdk5 (Fig. 3a). Because cdk5 is active primarily in neurons (Ino *et al.* 1994), associates with MTs indirectly through interactions with a MT-binding repeat of non-phosphorylated tau (Sobue *et al.* 2000), and its phosphorylation of tau directly leads to MT destabilization (Evans *et al.* 2000), we primarily focused upon the potential of taxol in regulating the activity of this tau kinase.

Neurons were treated with $A\beta_{25-35}$ in the absence and presence of 100 nM taxol for 4 days, whole cell lysates were prepared and cdk5 was immunoprecipitated. To assess cdk5 activity, the isolated immune-complexes were incubated in kinase buffer in the presence of [γ-^{32}P]ATP and either histone H1 or bovine brain tau as an *in vitro* substrate. $A\beta_{25-35}$ induced a 1.5-fold increase in cdk5-mediated tau phosphorylation that was completely prevented by taxol treatment (Fig. 3a); it is important to note that the modest increase in total cdk5 activity in whole cell lysates is likely due to $A\beta_{25-35}$ preferentially activating only the cytosolic pool of cdk5/p25 complexes (see below).

To determine if taxol may decrease cdk5 activity by directly inhibiting the enzyme, cdk5 was immunoprecipitated from untreated neurons and an *in vitro* kinase assay was performed as above except that 100 nM taxol was added directly to the reaction mix prior to initiating the reaction by the addition of substrate. Under these conditions, taxol had absolutely no effect on the phosphorylation of histone H1 or tau by cdk5 (Fig. 3b). These data suggest that the reversal of the Aβ-induced increase in cdk5 activity by taxol is not due to a direct inhibition of the kinase by the drug and requires cell signaling events. To examine the relationship between MT stabilization and the inhibitory effect of taxol on Aβ-induced cdk5 activation, neurons were treated with 10-deacetylbaccatin III. After 4 days of treatment, the cells were harvested, cdk5 activity immunoprecipitated and kinase activity assessed using histone H1 as the substrate. In contrast to taxol treatment, 10-deacetylbaccatin III had no effect on inhibiting Aβ-induced cdk5 activation (Fig. 3c).

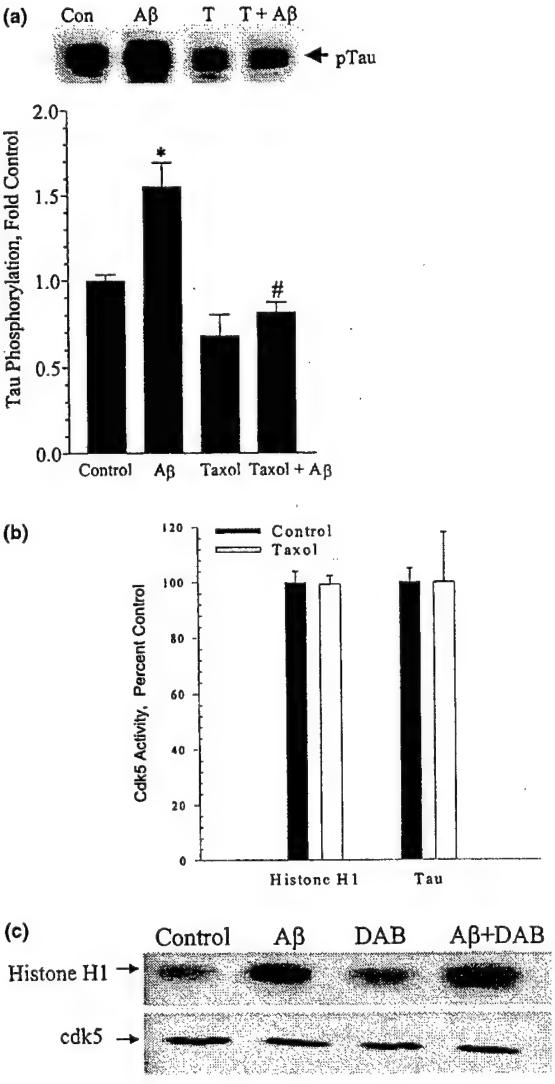

Fig. 3 Taxol but not 10-deacetylbaccatin III inhibits Aβ-induced cdk5 activation. Neurons were exposed for 4 days to buffer (Con), 100 nM taxol (T) or 10 μM $A\beta_{25-35}$ in the absence (Aβ) or presence of taxol (T + Aβ) and cell lysates were prepared. (a) Cdk5 was immunoprecipitated from whole cell lysates and kinase activity was assessed using tau as the substrate. Inset shows representative autoradiogram for the effect of $A\beta_{25-35}$ and taxol treatment on *in vitro* tau phosphorylation. Tau phosphorylation was quantitated from four experiments. *, $p < 0.01$ compared with control; #, $p < 0.001$ compared with $A\beta_{25-35}$ only. (b) Cdk5 was immunoprecipitated from untreated neurons and kinase activity assessed in the absence or presence of 100 nM taxol. Taxol was added directly to the reaction mixture prior to the addition of histone H1 or tau, the radiolabeled products were separated by electrophoresis and the level of phosphorylation determined using a phosphoimager. Results shown are mean ± SEM from three experiments. (c) Cells were incubated for 4 days with buffer (Control), 100 nM 10-deacetylbaccatin III (DAB) or 10 μM $A\beta_{25-35}$ in the absence (Aβ) or presence of 100 nM 10-deacetylbaccatin III (Aβ + DAB). Cells were harvested and cdk5 activity assessed as described above using histone H1 as the substrate. Upper panel shows histone H1 phosphorylation and bottom panel shows equivalent levels of cdk5 in each sample.

These results suggest that MT stabilization is necessary for the inhibitory effect of taxol on cdk5 activation by $A\beta_{25-35}$.

Cdk5 activity is regulated by interaction with specific activator proteins, p35 and p25, that have different subcellular localizations. Due to the presence of an N-terminal myristoylation site, p35 is essential for targeting cdk5 to the plasma membrane (Tsai *et al.* 1994; Dhavan *et al.* 2001). In contrast, a calpain-directed proteolytic degradation of p35 releases p25 from the N-terminal region of p35 that is tethered to the membrane and increases the amount of cytosolic cdk5/p25 complexes (Kusakawa *et al.* 2000; Lee *et al.* 2000; Nath *et al.* 2000). Because the above experiments used an antibody directed against cdk5, we could not determine whether $A\beta_{25-35}$ activated cdk5/p35 or cdk5/p25 complexes nor whether one or both complexes may be inhibited by taxol.

To determine the effect of $A\beta_{25-35}$ and taxol on the activity of cdk5/p35 versus cdk5/p25 complexes, two approaches were taken. In the first approach, cdk5 activity was assessed following immunoprecipitation with antibodies that recognize either the N-terminus (N-20) or C-terminus (C-19) of p35. As p35 and p25 share the same C-terminus, the C-19 p35 antibody will immunoprecipitate both p35 and p25 and provide an assessment of total cdk5 activity. However, the N-20 p35 antibody is directed against an N-terminus region that is lacking in p25 and provides a measure of kinase activity associated with only the cdk5/p35 complex. Therefore, the contribution of the cdk5/p25 complex to total cdk5 activity may be measured indirectly by subtracting the cdk5/p35-specific activity (N-20 antibody) from the total activity (cdk5/p35 + cdk5/p25) obtained following immunoprecipitation with the C-19 antibody.

Neurons were treated with $A\beta_{25-35}$ in the absence or presence of taxol, the cells were harvested in lysis buffer and each whole cell lysate was divided into two × 100 μg aliquots. Each aliquot was then incubated with 2 μg of the C-19 or the N-20 p35 antibody, the immune complexes were isolated with protein A Sepharose and cdk5 activity was assessed as described above. Similar to results in Fig. 3a, $A\beta_{25-35}$ treatment activated total cdk5 activity (C-19 p35 antibody) but kinase activity associated with the cdk5/p35 complex (N-20 p35 antibody) did not contribute to the overall increase (Fig. 4a). Indeed, total cdk5 was activated by $A\beta_{25-35}$ about 1.5-fold. However, subtracting the p35-specific activity from total activity indicated that cdk5/p25 complexes were activated by $A\beta_{25-35}$ approximately 2.1–2.3-fold (Fig. 4b). Moreover, taxol significantly inhibited kinase activity associated with the cdk5/p25 complexes but had no effect on the activity of cdk5/p35 complexes (Fig. 4b).

To provide a more direct assessment of the effect of $A\beta_{25-35}$ and taxol on the activity of cdk5/p25 complexes, our second approach exploited the differential compartmentation of cdk5/p35 versus cdk5/p25 complexes. As cdk5/p35 is primarily membrane-associated whereas cdk5/p25 is cytosolic (Nikolic and Tsai 2000), soluble and particulate fractions of treated neurons were prepared as described in Experimental procedures. Prior to centrifugation, an aliquot of the whole cell lysate was removed to determine total cdk5 activity. Cdk5 present in the whole cell lysate, soluble and particulate fractions was immunoprecipitated with the C-19 p35 antibody and kinase determined as described above. Once again, $A\beta_{25-35}$ activated total cdk5 activity immunoprecipitated from whole cell lysates by 1.5-fold and this activation was completely inhibited by taxol (Fig. 4c). However, cdk5/p25 activity immunoprecipitated from the cytosolic fraction was activated greater than 3-fold by $A\beta_{25-35}$ and this activation was inhibited by about 55% in cells treated with taxol and $A\beta_{25-35}$. Similar to our results above, $A\beta_{25-35}$ and taxol had no effect on the activity of cdk5/p35 complexes immunoprecipitated from the membrane fraction. Together, these results strongly support that Aβ-induced cdk5 activity is associated primarily with cytosolic cdk5/p25 complexes and that taxol specifically decreases the Aβ-induced activation of the cdk5/p25 complex.

Taxol prevents Aβ-induced changes in the ratio of p35/25

Because taxol was specifically inhibiting the activity of cdk5/p25 complexes, we next addressed potential mechanisms for this effect. p35 is a short-lived protein that undergoes relatively rapid degradation by calpain-mediated proteolysis (Lee *et al.* 2000) and via interaction with the proteasome (Patrick *et al.* 1998). Moreover, recent reports suggest that Aβ increases the degradation of p35 to p25 in AD brain (Lee *et al.* 1999; Patrick *et al.* 1999) and cultured primary neurons (Lee *et al.* 2000). Similarly, $A\beta_{25-35}$ treatment induced a significant 1.5-fold increase in the production of p25 in the cortical neurons after 4 days (Fig. 5a) and co-treatment of the cells with $A\beta_{25-35}$ and taxol completely prevented this increase. Thus, decreased p25 production correlated with the effect of taxol on decreasing cdk5/p25 activity.

To determine if taxol was decreasing the turnover of p35, we measured its half-life in cortical neurons treated with vehicle or 100 nM taxol for 4 days. To inhibit protein synthesis, 30 μg/mL of cycloheximide was added to the cells (Patrick *et al.* 1998) and the neurons were scraped into lysis buffer at various times between 0 and 480 min following the addition of cycloheximide. Similar amounts of total protein from each time point were separated by SDS–PAGE, the proteins were transferred to nitrocellulose and the presence of p35 and p25 was determined by immunoblot analysis using the C-19 p35 antibody. In control neurons the half-life of p35 was around 140–160 min (Fig. 5b and c), substantially longer then the 20–30 mins that has been reported in cortical neurons cultured for 3 days *in vitro* (Patrick *et al.* 1998) or in transfected COS-7 cells (Patrick *et al.* 1999). Whether this difference is related to the age of the cultures, specific

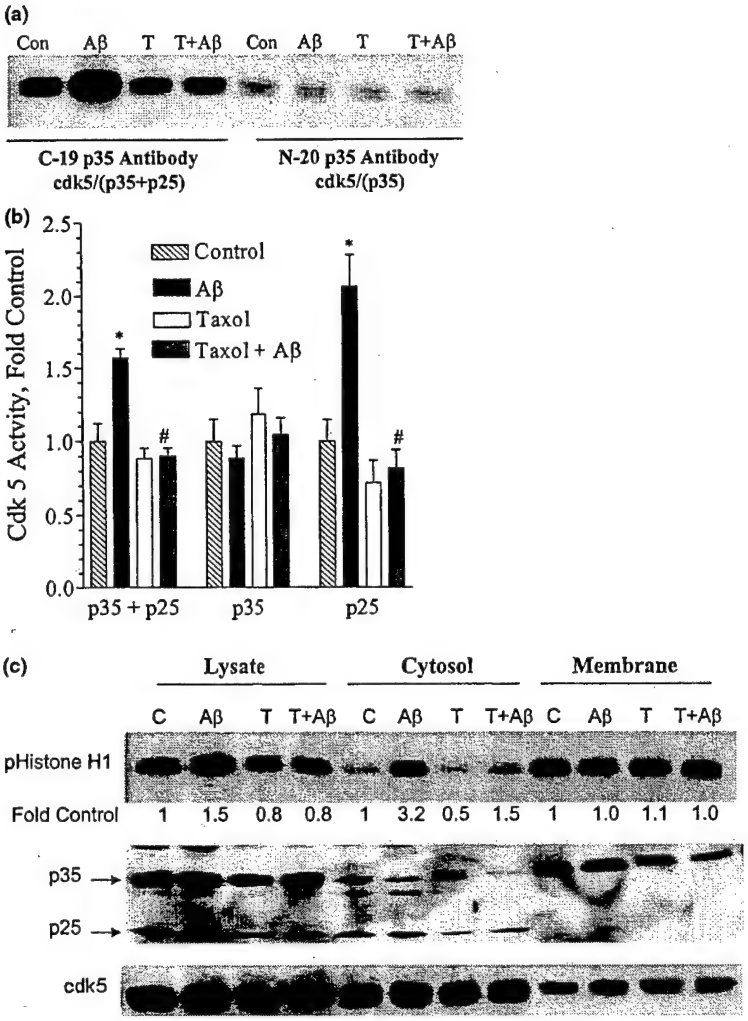

Fig. 4 Taxol inhibits the activity of cdk5/p25 complexes. (a) Neurons were treated as indicated and the whole cell lysates were divided into 2 × 100 μg aliquots. Cdk5 was immunoprecipitated from each aliquot with either the C-19 p35 antibody which recovers cdk5/(p35 + p25) complexes or the N-20 p35 antibody which recovers only cdk5/p35 complexes. Cdk5 activity was assayed and phosphorylated histone H1 separated by SDS–PAGE and detected by phosphoimaging. (b) The relative density of histone H1 phosphorylation by cdk5(p35 + p25) and cdk5/(p35) complexes was quantitated from three experiments. Results shown for cdk5/(p25) were obtained by subtracting the relative density of histone H1 phosphorylation obtained for cdk5/(p35) (5.4 ± 0.8) from cdk5/(p35 + p25) (13.5 ± 1.6) and expressed as fold control. *, $p < 0.01$ compared to control; #, $p < 0.001$ compared to Aβ only. (c) Neurons were treated as indicated and an aliquot of the total lysate saved. Of the remaining whole cell lysates, 100 μg was separated into cytosolic and membrane fractions by centrifugation. Each fraction was immunoprecipitated with the C-19 p35 antibody and cdk5 activity assessed using histone H1 as the substrate. Upper panel, histone H1 phosphorylation; middle panel, immunoblot of p35 and p25 levels in membrane and cytosolic fractions; lower panel, immunoblot for the level of cdk5 in each sample.

differences in culture conditions, antibodies or cell type is unknown. Nevertheless, addition of 100 nM taxol to the cortical neurons for 4 days increased the half-life of p35 to about 320–340 min (Fig. 5b and c). Importantly, using the same cell extracts, taxol had no effect on the half-life of either tau or cdk5, indicating that it was not non-specifically decreasing protein degradation (Fig. 5d). The lack of change in cdk5 and tau levels also indicates that the increased half-life of p35 in the presence of taxol is not due to differences in protein loading.

Phosphorylation of p35 by cdk5 enhances its degradation via the proteasome and direct inhibition of cdk5 with roscovitine can increase the half-life of p35 (Patrick *et al.* 1998). Therefore, a decrease in cdk5 activity would be

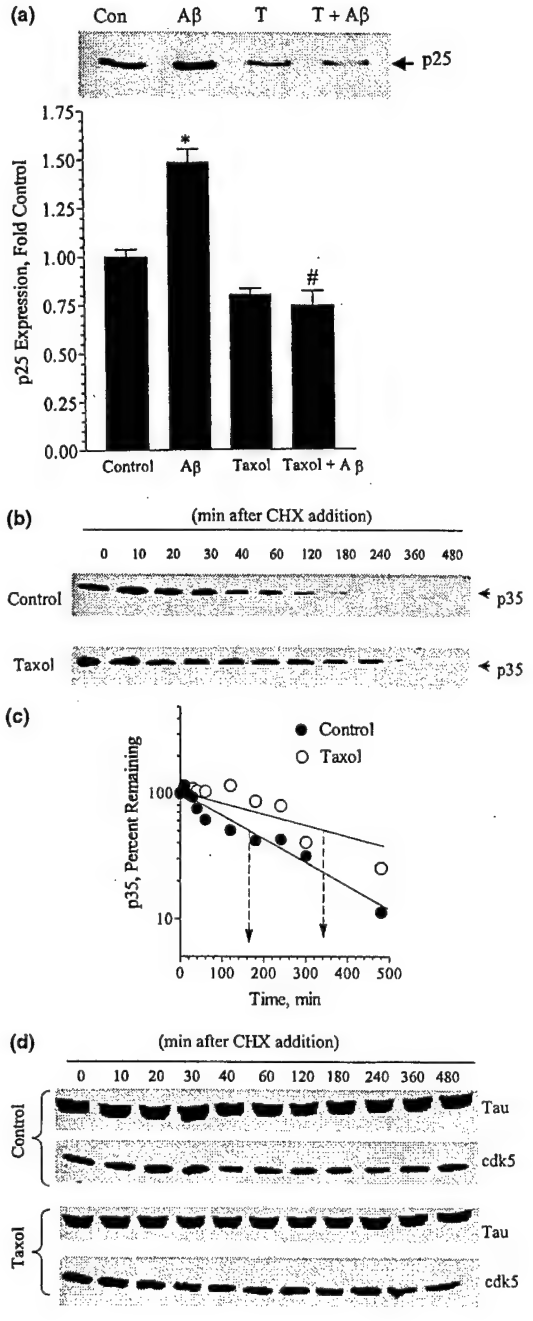

Fig. 5 Taxol increases the half-life of p35 and decreases the formation of p25 by $A\beta_{25-35}$. (a) Neurons were exposed for 4 days to buffer (Con), 100 nM taxol (T) or 10 μM $A\beta_{25-35}$ in the absence (Aβ) or presence of taxol (T + Aβ), cell lysates were prepared and p25 levels were determined by immunoblot analysis. Inset shows representative immunoblot for the effect of $A\beta_{25-35}$ and taxol treatment on p25 expression. p25 expression was quantitated densitometrically from four experiments. *, $p < 0.001$ compared with control; #, $p < 0.001$ compared with Aβ only. (b) Neurons were treated with vehicle or 100 nM taxol for 4 days, 30 μg/mL cycloheximide (CHX) was added, and the cells were harvested at the indicated time after CHX addition. Whole cell lysates were subjected to SDS–PAGE (20 μg per lane) and the half-life of p35 was measured by immunoblot analysis. (c) Expression of p35 was quantitated by densitometry and the approximate half-life of p35 in control and taxol treated cells is indicated by the arrows. (d) Separate aliquots from the same neuronal lysates used above were subjected to SDS–PAGE and the effect of taxol on the half-life of tau and cdk5 was determined by immunoblot analysis.

expected to increase the half-life of p35. However, our results indicate that taxol does not directly inhibit cdk5, suggesting that it stabilizes p35 by another mechanism. Although we cannot rule out the possibility that taxol may increase the half-life of p35 by interfering with its accessibility to serve as a substrate for cdk5, the calpain-mediated cleavage of p35 also leads to enhanced formation of p25 (Kusakawa *et al.* 2000; Lee *et al.* 2000). Because taxol stabilized p35 and decreased p25 formation, we examined the effect of $A\beta_{25-35}$ and taxol on calpain activity. Primary cortical neurons were treated with $A\beta_{25-35}$ in the absence or presence of taxol for 4 days, cell lysates were prepared and calpain activity was determined fluorometrically (Xie and Johnson 1997). As anticipated, $A\beta_{25-35}$ treatment induced an approximate 2-fold activation of calpain (Fig. 6). Although taxol decreased basal calpain activity, it also inhibited calpain activation induced by $A\beta_{25-35}$. As a positive control, the assay was verified by incubating the cell lysate with ALLN, a calpain inhibitor that completely blocked hydrolysis of the substrate.

The inhibition of calpain activity by taxol was not due to decreases in the level of calpain-1 (μ-calpain) or calpain-2 (m-calpain) nor to increases in the expression of the endogenous calpain inhibitor, calpastatin (data not shown). It should be noted, however, that 13 different calpains are broadly expressed (Huang and Wang 2001). Importantly, taxol had no effect on endogenous calpain activity when it was added directly to cell lysates prepared from untreated neurons and incubated with the calpain substrate. This result suggests that taxol does not inhibit calpain directly. However, to rule out the possibility that some endogenous proteins or lipids present in the cell lysate were sequestering taxol and preventing it from inhibiting calpain directly, purified calpain-1 was incubated with the peptide substrate plus 5 mM Ca^{2+} in the presence and absence of 100 nM taxol. Once again, taxol had no inhibitory effect on calpain-1 activity with the purified enzyme (data not shown). Collectively, these results suggest that a primary point of action of taxol is upstream of calpain activation by $A\beta_{25-35}$.

Overexpression of p25 reverses taxol-mediated neuroprotection against Aβ-induced cell death

Transgenic mice overexpressing p25 exhibit cytoskeletal disruptions and increased phosphorylation of neurofilaments

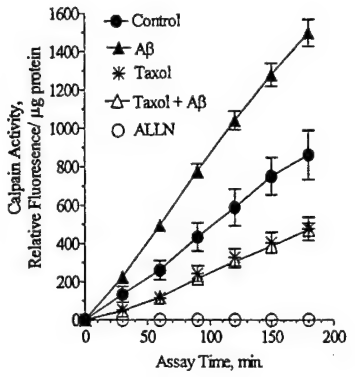

Fig. 6 Inhibition of Aβ-induced calpain activation by taxol. Neuronal cultures were exposed for 4 days to 10 μM $A\beta_{25-35}$ in the absence or presence of 100 nM taxol and cell lysates prepared. Calpain activity was monitored fluorometrically in quadruplicate and the results shown are from four experiments.

and tau (Ahlijanian *et al.* 2000). Moreover, tau phosphorylation by cdk5 decreases MT stability (Lee *et al.* 2001). If MT stabilization by taxol is sufficient to protect neurons against Aβ toxicity, then it should be protective even during ectopic expression of p25 and increased tau phosphorylation. Primary cortical neurons were infected with a recombinant p25 adenovirus and protein expression and cdk5 activity determined over a period of 4 days. Overexpression of p25 was maximal 2 days after infection (Fig. 7a) and increased cdk5 activity about 2-fold using either histone H1 or tau as the substrate (Fig. 7b). Therefore, we examined the effect of p25 overexpression (200 pfu/cell) on the protection against $A\beta_{25-35}$ toxicity by taxol at this time.

Similar to uninfected cells (Fig. 5a), taxol inhibited the Aβ-induced increase in p25 expression (Fig. 7c, upper panel) and cdk5-mediated tau phosphorylation (Fig. 7c, middle panel) in cells infected with the blank virus. In contrast, neither $A\beta_{25-35}$ nor taxol changed p25 expression (Fig. 7c, upper panel) or cdk5-mediated histone H1 phosphorylation (Fig. 7c, middle panel) in neurons infected with the p25 adenovirus. As taxol did not decrease cdk5 activity in cells overexpressing p25, these results also support that the inhibitory effect of taxol on Aβ-induced cdk5 activation requires the disruption of signal transduction events and is not due to a direct inhibition of the kinase by taxol.

$A\beta_{25-35}$ induced a significant level of cell death in neurons infected with blank or p25 adenoviruses (Fig. 7d). However, p25 overexpression only modestly decreased cell viability regardless of the absence or presence of $A\beta_{25-35}$. The modest effect of p25 expression on increasing the extent of cell death may be due to using these cells 2 days post infection. At this time, the viability of neurons infected with blank virus (71 ± 3.1%) was similar to uninfected neurons (76.6 ± 2.6%). Although p25 expression was significantly more effective at inducing cell death 3–4 days post infection, viability of neurons treated with blank virus alone was also decreasing (data not shown). Importantly, viral infection did not non-specifically alter the response to taxol as the drug also protected against $A\beta_{25-35}$ toxicity in neurons infected with blank virus (compare bars 3 and 7). In contrast, taxol did not significantly inhibit cell death in response to increased p25 expression in the absence (compare bars 2 and 6) or presence (compare bars 4 and 8) of $A\beta_{25-35}$. Indeed, forced expression of p25 reversed the neuroprotective effect of taxol seen in cells infected with blank virus and treated with $A\beta_{25-35}$ (compare bars 7 and 8). As ectopic expression of p25 had no effect on the stabilization of MTs by taxol (data not shown), these data suggest that MT stabilization alone is not sufficient to overcome the detrimental effect of enhanced cdk5 activity.

Systemic administration of a taxol analog mimics the effect of taxol on inhibiting activation of cdk5 by $A\beta_{25-35}$

Unfortunately, identifying the most active compound in cell cultures with regards to MT stabilization, intracellular signaling and neuroprotection is usually not sufficient to overcome the difficulties of showing activity in an intact organism. In this regard, the potential for taxol as a therapeutic agent either for AD or cancers of the central nervous system (CNS) is limited by its lack of penetration across the blood–brain barrier.

The blood–brain barrier is composed of numerous tight junctions between capillary endothelial cells that create a low passive permeability across this barrier and a selective exchange of molecules from the circulation into the CNS (Thiel and Audus 2001). Additionally, the presence of the P-glycoprotein in cells forming the blood–brain barrier permits the rapid efflux of lipophilic molecules such as taxol which limits the effectiveness of this drug in treating tumors of the CNS (Heimans *et al.* 1994; Brouty-Boye *et al.* 1995). Although pharmacologic inhibition of this efflux can increase the brain level of taxol 4-fold (van Asperen *et al.* 1997), transport of essential macromolecules across the blood–brain barrier may also be facilitated by highly selective transporter proteins (Thiel and Audus 2001). The presence of specific small molecule transporters offers the possibility that modification of taxol may circumvent P-glycoprotein-mediated efflux and enhance its permeability across the blood–brain barrier while retaining its MT-stabilizing and neuroprotective properties.

Using combinatorial chemistry and a strategy that exploited the presence of specific transporters for basic amino acids, biotin, amines and monocarboxylic acids, a library of compounds was prepared that modified taxol with these various molecules (Liu *et al.* 2002). From this library, a succinylated taxol derivative (10-succinyl taxol, TX67) emerged as a candidate molecule that efficiently stabilized MTs (Liu *et al.* 2002), bypassed the P-glycoprotein efflux system and has a 150-fold greater permeability than taxol at

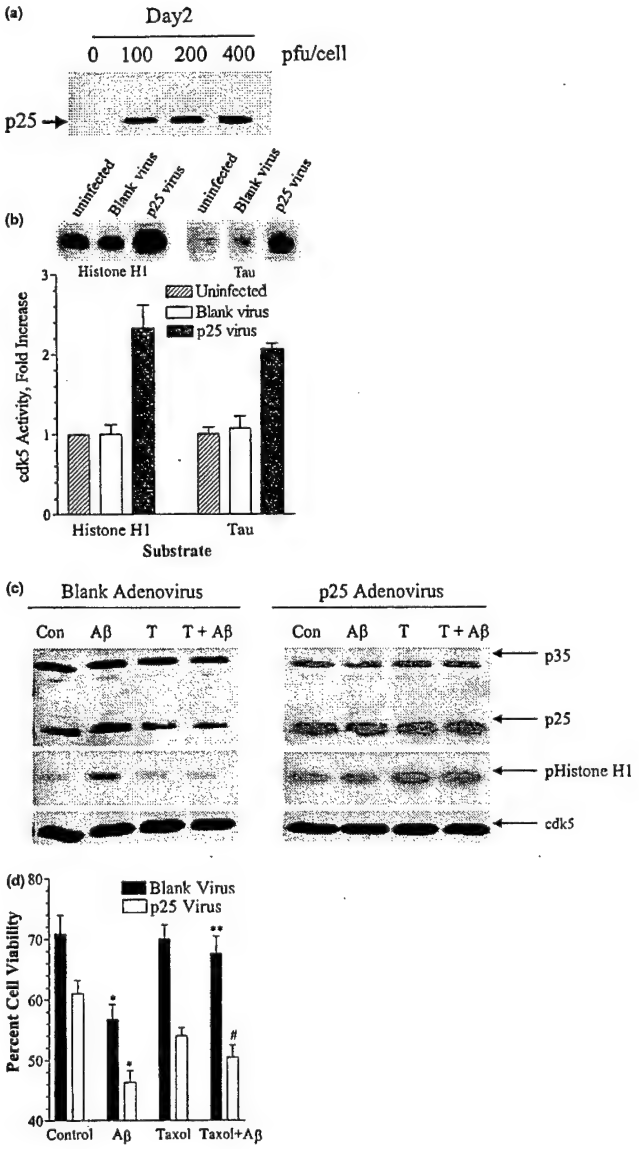

Fig. 7 Overexpression of p25 reverses the neuroprotective effect of taxol. (a) Neurons were infected with recombinant adenoviruses at 0–400 pfu/cell for 2 days and cell lysates were prepared. Following SDS-PAGE (20 μg/lane), p25 was detected by immunoblot analysis. (b) Cell lysates were prepared from uninfected neurons or neurons infected with 200 pfu/cell of blank adenovirus or p25 adenovirus for 2 days. Cdk5 was immunoprecipitated and its activity was assessed using histone H1 or tau as the substrate in an *in vitro* kinase assay. The upper panels show the extent of histone and tau phosphorylation. Band intensity was quantitated using a phosphoimager and expressed as fold-increase relative to basal activity of uninfected cells. The results from three experiments are shown. (c) Neurons were infected with blank or p25 adenoviruses at 200 pfu/cell. After 2 h, the neurons were treated with buffer (Con), 100 nM taxol (T) or 10 μM $A\beta_{25-35}$ in the absence (Aβ) or presence of taxol (T + Aβ) for 2 days. Cell lysates were prepared and p25 levels were assessed by immunoblot analysis. Cdk5 (C-8 antibody) was immunoprecipitated and its activity assessed using histone H1 as the substrate. Total cdk5 levels (lower panel) were similar between each treatment. (d) Cells infected with blank or p25 adenovirus were treated with 10 μM $A\beta_{25-35}$ in the absence or presence of 100 nM taxol for 2 days and cell viability was assessed. Values presented are from four experiments. The per cent viability in uninfected neuronal cultures was 76.6 ± 2.6. *, $p < 0.05$ for Aβ compared to respective control; **, $p < 0.05$ blank virus-taxol compared with blank virus-(taxol + Aβ); #, $p < 0.001$ blank virus-(taxol + Aβ) compared with p25 virus-(taxol + Aβ).

therapeutically relevant concentrations in a cellular model for the blood–brain barrier (Michaelis *et al.* 2002). Importantly, TX67 also was neuroprotective against Aβ in cultured primary neurons (Table 1). Therefore, we assessed whether systemic administration of TX67 may mimic the effect of taxol on inhibiting Aβ-induced cdk5 activation in acutely dissociated neurons prepared from TX67-treated animals. Adult mice were injected every other day for 16 days with vehicle, 8 mg/kg of TX67 or a similar dose of taxol. To determine the *in vivo* effectiveness of TX67 versus taxol, cultures of acutely dissociated cortical neurons were prepared and the cells were treated *ex vivo* with buffer or 20 μM $A\beta_{25-35}$ immediately after their preparation. We used a higher concentration of $A\beta_{25-35}$ in these studies as the acutely dissociated neurons are still partially clumped and represent a mixed population of cells. After 24 h, the cells were harvested, cdk5 was immunoprecipitated and histone H1 phosphorylation was assessed using the *in vitro* kinase assay. Similar to the cultured embryonic cortical neurons, $A\beta_{25-35}$ induced a 1.8-fold increase in cdk5 activity in acutely dissociated neurons obtained from adult animals that received the drug vehicle only (Fig. 8a). Administration of taxol to the animals was ineffective at preventing the Aβ-induced activation of cdk5, consistent with its poor ability to cross the blood–brain barrier (Cavaletti *et al.* 2000). In contrast, TX67 markedly decreased the magnitude of basal cdk5 activity and blocked its activation by $A\beta_{25-35}$ (Fig. 8a and b). Overall, these data provide compelling evidence for proof of principle that taxol analogs may be useful for attenuating the magnitude of some aspects of Aβ signal transduction *in vivo*.

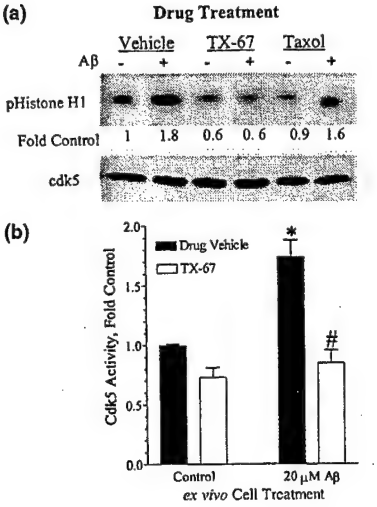

Fig. 8 Systemic administration of a succinylated taxol analog (TX67) blocks Aβ-induced cdk5 activation. (a) Animals were given intraperitoneal injections of the drug vehicle, 8 mg/kg TX 67 or taxol every other day for 16 days. The animals were killed, cultures of acutely dissociated cortical neurons were prepared and treated with 20 μM $A\beta_{25-35}$ for 24 h. Cell lysates were prepared, cdk5 was immunoprecipitated and its activity was assessed using histone H1 as the substrate (upper panel). The amount of cdk5 in each sample was determined by immunoblot analysis (lower panel). Histone H1 phosphorylation was quantitated with a phosphoimager and normalized to the expression level of cdk5 to account for the slight differences in cdk5 levels between samples. Numbers below the upper panel indicate fold histone H1 phosphorylation relative to control neurons obtained from animals receiving the drug vehicle. (a) Quantitation of the effect of TX-67 administration on Aβ-induced histone H1 phosphorylation. Values are from three animals for each treatment. *, $p < 0.01$ compared with control neurons from animals receiving the drug vehicle; #, $p < 0.01$ compared with Aβ-treated neurons from animals receiving the drug vehicle.

Discussion

Lee and colleagues originally proposed that MT stabilizing agents may be useful therapeutics for slowing the progression of the neurofibrillary pathology that is one hallmark of advanced AD (Lee *et al.* 1994). In this report, we provide insight into the molecular mechanism by which taxol protects cortical neurons from toxicity by Aβ peptides. Although taxol stabilized MTs in $A\beta_{25-35}$ treated cells, it also decreased Aβ-induced calpain activation, p25 production and activation of cdk5/p25 complexes. Collectively, these results suggest that taxol acts upstream of calpain in regulating the cdk5 pathway.

The cdk5/p25 complex as a therapeutic target in AD

The induction of tau hyperphosphorylation by cdk5/p25 complexes in cultured cells and transgenic mice suggests that this complex may contribute to the increased amount of hyperphosphorylated tau present in PHFs from AD patients (Dhavan *et al.* 2001). Increased cdk5 activity may also provide a mechanistic link in the etiology of motor neuron dysfunction in amyotrophic lateral sclerosis (Nguyen *et al.* 2001; Patzke and Tsai 2002b). Thus, the cdk5/p25 complex is emerging as an attractive pharmacological target in neurodegenerative diseases.

Direct inhibition of cdk5 with kinase inhibitors can prevent Aβ-induced cell death of primary hippocampal neurons (Alvarez *et al.* 1999) and our results are consistent with these data. However, taxol did not inhibit cdk5 activity directly but decreased kinase activity, presumably by regulating the formation of p25. These data suggest that the pharmacologic regulation of p25 production may provide an alternative therapeutic approach to regulating cdk5 activity. Although a calpain inhibitor would obviously be attractive for preventing this degradation, calpain is critical to regulating cytoskeletal proteins and numerous metabolic functions in cells. This broad spectrum of bioactivity contributes to the considerable lack of specificity and toxicity that current calpain inhibitors exhibit toward cells (Nakagawa and Yuan 2000; Wang 2000; Huang and Wang 2001).

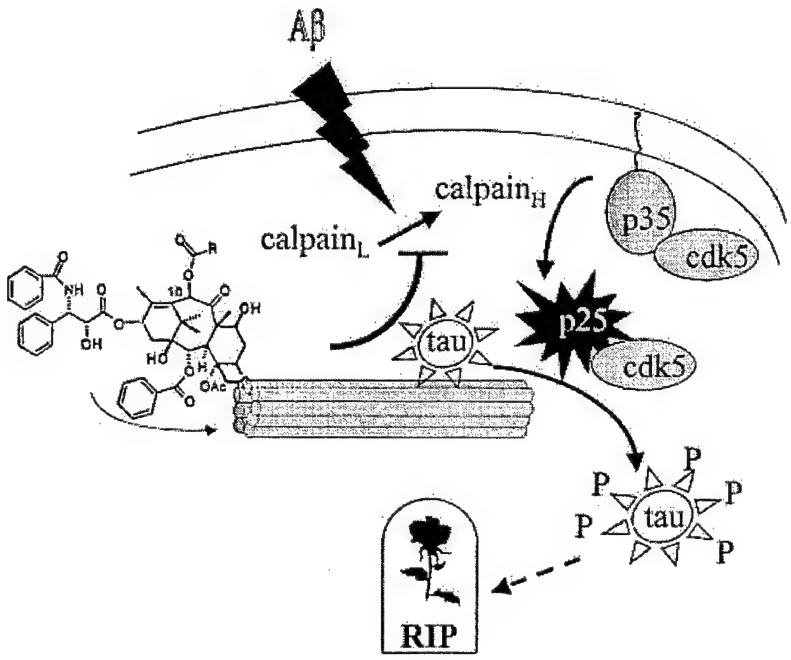

Fig. 9 Taxol inhibition of the cdk5 pathway occurs at the level of calpain activation by Aβ. See text for details. Calpain$_L$-low activity; calpain$_H$- high activity. The R group at the C10 position contains an acetyl moiety in taxol and this group is substituted with succinate in TX-67.

A caveat to the potential of cdk5 as a therapeutic target, with respect to AD at least, hinges upon whether enhanced production of p25 and chronic activation of cdk5 activity is a consistent phenomenon in AD brain. Recent studies from post-mortem brain tissue obtained from AD patients suggest that p25 levels may be elevated in this disease (Patrick *et al.* 1999, 2001). Consistent with increased p25 expression, prefrontal cortex from post-mortem brain of AD patients showed a significant increase in cdk5 activity relative to control patients, when corrected for either the level of cdk5 expression or for neuronal loss (Lee *et al.* 1999). In contrast, others have reported that p25 levels were decreased in post-mortem tissue from AD versus control brain (Taniguchi *et al.* 2001; Yoo and Lubec 2001). One complicating factor that may contribute to these discrepancies is the effect of the post-mortem interval on induction of an artifactual increase in p25 production via calpain-mediated degradation (Kusakawa *et al.* 2000; Taniguchi *et al.* 2001). Thus, a critical assessment using either pharmacologic or genetic manipulation of the cdk5 pathway in animals and examination of its role in the development of neurofibrillary pathology will be required to characterize more fully the role of this pathway in AD.

Taxanes and neurodegenerative disease: the conundrum of multiple mechanisms-multiple outcomes

Increased tau phosphorylation by cdk5 is sufficient to directly decrease stabilization of MTs and contribute to Aβ toxicity (Evans *et al.* 2000). MT-stabilization by taxol, and presumably taxol analogs, is necessary for neuroprotection against Aβ toxicity as 10-deactylbaccatin III does not stabilize MTs and was ineffective at preventing Aβ-induced cell death. Further, MT stabilization is also necessary for the inhibition of the cdk5 pathway by taxol as 10-deacetylbacctin III did not inhibit the activation of cdk5 by $A\beta_{25-35}$. However, MT stabilization alone was not sufficient to protect neurons against $A\beta_{25-35}$ toxicity in neurons ectopically expressing p25. Similarly, activation of c-*jun* N-terminal kinase (JNK) by taxol in breast cancer cells also requires MT binding (Wang *et al.* 1998) and no clear evidence exists that any effect of taxol on cell signaling is necessarily independent of its MT binding properties at therapeutically relevant concentrations (Blagosklonny and Fojo 1999). Together, these data support the hypothesis that the state-of-stability or dynamic instability of axonal MTs represents a signaling pathway within neurons and that the integrity of MT structure may serve as a sensor of the normal homeostasis in cells. A schematic summary of the role of taxanes in regulating Aβ toxicity is presented in Fig. 9. We propose that taxol may minimize Aβ toxicity through distinct but interrelated contributions: (i) its ability to stabilize MTs in the presence of Aβ and (ii) an inhibition of Aβ-induced calpain activation which minimizes proteolysis of p35 to p25, leading to decreased activation of cdk5/p25 complexes and subsequent tau phosphorylation. Finally, as Aβ induces the loss of intraluminal Ca^{2+} pools in the endoplasmic reticulum (ER) (Siman *et al.* 2001), the inhibition of calpain by taxol raises the possibility that MT-stabilization may link to minimizing ER stress. We are currently examining the role of taxol and the cdk5 pathway in regulating the activity of ER-resident proteins such as presenilins and caspase 12; the later is

activated by calpain cleavage and is critical to Aβ -induced apoptosis (Nakagawa and Yuan 2000; Yoneda *et al.* 2001).

An important consideration in our approach of using taxol and taxol analogs as neuroprotective agents derives from the likelihood that these compounds may affect other aspects of cell signaling (Blagosklonny and Fojo 1999). Taxol is well recognized as an anti-mitotic agent that induces apoptosis in cancer cells by causing cell cycle arrest at the G2/M transition (Jordan *et al.* 1993; Blagosklonny and Fojo 1999), activating JNK (Wang *et al.* 1998; Amato *et al.* 1998) and inducing phosphorylation of bcl-2 (Blagosklonny *et al.* 1996; Blagosklonny *et al.* 1997). Additionally, in macrophages and monocytes, taxol exerts lipopolysaccharide-like effects at high concentrations (10–30 μM) (Ding *et al.* 1990; Manthey *et al.* 1993), which, although therapeutically unsustainable (Blagosklonny and Fojo 1999), may contribute to its apoptotic actions.

It has been reported recently that 100 nM taxol can also induce apoptosis in cortical neurons through a pathway independent of bcl-2 phosphorylation but still requiring activation of a nuclear pool of JNK and phosphorylation of the c-*jun* transcription factor (Figueroa-Masot *et al.* 2001). In contrast, addition of 1–10 μM taxol had no effect on neuronal morphology and presumably the viability of hippocampal neurons obtained from wild type or tau-deficient mice (Rapoport *et al.* 2002). Indeed, taxol had no significant effect on the activation of caspase 3 and significantly decreased the Aβ-induced activation of this enzymatic marker of apoptosis (Michaelis *et al.* 1998). Although we have not examined the effect of taxol on neuronal viability under the conditions used by Xia and colleagues (Figueroa-Masot *et al.* 2001), it is possible that the addition of 10% fetal calf serum to the primary cultures used in these studies may provide very strong survival signals upon which the neurons become dependent. Under these growth conditions, taxol may promote apoptosis by stabilizing MTs and decreasing the activity of phosphoinositide 3-kinase (Figueroa-Masot *et al.* 2001).

Similar to our results, a recent study also found that taxol did not induce death in neurons isolated from wild type or tau-deficient animals in the absence of Aβ treatment (Rapoport *et al.* 2002). However, taxol was not protective against Aβ treatment of neurons from wild type animals. Interestingly, neurons from tau-deficient animals were insensitive to Aβ-induced neurite degeneration *unless* the MTs were first stabilized with taxol. These results have led to the proposal that increasing MT stability may not permit cells to compensate for degenerative cues arising from Aβ treatment (Rapoport *et al.* 2002). The reason for the underlying difference between the protective effect of taxol against Aβ peptides in our study versus Rapoport *et al.* (2002) is unclear but both studies support that tau plays a central role in regulating cellular responses to Aβ peptides. Nevertheless, the rather dichotomous effect of taxol on post-mitotic neurons under different growth conditions raises the issue that the *in vivo* effects of taxol at therapeutically sustainable concentrations (5–200 nM) (Blagosklonny and Fojo 1999) may be influenced by the balance between survival and stress signals that impact on the state-of-stability or dynamic instability of axonal MTs in a given neuronal population.

The *in vivo* potential of MT-stabilizing agents to minimize neurofibrillary pathology

Numerous lipophilic drugs, including taxol, do not penetrate the blood–brain barrier due to the presence of a P-glycoprotein efflux system, the multidrug resistant protein (MDR1) (Teraski and Tsuji 1995). We circumvented this problem by using a succinylated taxol analog that is not effluxed by P-glycoprotein present in the capillary endothelial cells that form the blood–brain barrier (Michaelis *et al.* 2002). Indeed, neurons obtained from TX67 but not taxol treated animals, showed decreased basal cdk5 activity and were resistant to the Aβ-induced activation of this tau kinase. This outcome suggests that, in contrast to the use of direct inhibitors of cdk5 that interact with the ATP binding domain (i.e. roscovitine), taxol analogs may permit an alternative regulation of cdk5 which may allow the enzyme to respond to cellular signals. In this regard, a basal level of cdk5 activity is associated with enhanced neuronal survival (Li *et al.* 2002).

In summary, our results support the premise that MT-stabilizing agents based upon the taxol backbone can be rationally designed and may have potential usefulness in treating neurofibrillary pathology if they cross the blood–brain barrier, stabilize MTs and attenuate tau kinase activity. If tau phosphorylation by cdk5 is sufficient to destabilize MTs (Evans *et al.* 2000), taxol analogs or other MT-stabilizing agents that are more permeable to the blood–brain barrier (i.e. epothilones) may minimize MT destabilization and prove beneficial in slowing the formation of NFTs during the progression of AD and other tauopathies.

Acknowledgements

We would like to thank Dr L-H. Tsai for providing p35 cDNA, Dr Peter Davies for the Tau-5 and PHF-1 antibodies, and Dr T. C. He for the pAdTRACK and pAdEASY adenoviral vectors. This work was supported by grants NS38154, NS38745 (RTD), H220528 (MLM) and CA82801 (GG) from the National Institutes of Health and the Institute for the Study of Aging (MLM).

References

Ahlijanian M. K., Barrezueta N. X., Williams R. D., Jakowski A., Kowsz K. P., McCarthy S., Coskran T., Carlo A., Seymour P. A., Burkhardt J. E., Nelson R. B. and McNeish J. D. (2000) Hyperphosphorylated tau and neurofilament and cytoskeletal disruptions in mice overexpressing human p25, an activator of cdk5. *Proc. Natl Acad. Sci. USA* **97**, 2910–2915.

Alvarez A., Toro R., Caceres A. and Maccioni R. B. (1999) Inhibition of tau phosphorylating protein kinase cdk5 prevents beta-amyloid-induced neuronal death. *FEBS Lett.* **459**, 421–426.

Alvarez A., Munoz J. P. and Maccioni R. B. (2001) A Cdk5-p35 stable complex is involved in the beta-amyloid-induced deregulation of Cdk5 activity in hippocampal neurons. *Exp. Cell Res.* **264**, 266–274.

Amato S. F., Swart J. M., Berg M., Wanebo H. J., Mehta S. R. and Chiles T. C. (1998) Transient stimulation of the c-Jun – NH2-terminal kinase/activator protein 1 pathway and inhibition of extracellular signal-regulated kinase are early effects in paclitaxel-mediated apoptosis in human B lymphoblasts. *Cancer Res.* **58**, 241–247.

van Asperen J., van Tellingen O., Sparreboom A., Schinkel A. H., Borst P., Nooijen W. J. and Beijnen J. H. (1997) Enhanced oral bioavailability of paclitaxel in mice treated with the P-glycoprotein blocker SDZ PSC 833. *Br. J. Cancer* **76**, 1181–1183.

Billingsley M. L. and Kincaid R. L. (1997) Regulated phosphorylation and dephosphorylation of tau protein: effects on microtubule interaction, intracellular trafficking and neurodegeneration. *Biochem. J.* **323**, 577–591.

Blagosklonny M. V. and Fojo T. (1999) Molecular effects of paclitaxel: myths and reality (a critical review). *Int. J. Cancer* **83**, 151–156.

Blagosklonny M. V., Schulte T., Nguyen P., Trepel J. and Neckers L. M. (1996) Taxol-induced apoptosis and phosphorylation of Bcl-2 protein involves c-Raf-1 and represents a novel c-Raf-1 signal transduction pathway. *Cancer Res.* **56**, 1851–1854.

Blagosklonny M. V., Giannakakou P., el Deiry W. S., Kingston D. G., Higgs P. I., Neckers L. and Fojo T. (1997) Raf-1/bcl-2 phosphorylation: a step from microtubule damage to cell death. *Cancer Res.* **57**, 130–135.

Brouty-Boye D., Kolonias D., Wu C. J., Savaraj N. and Lampidis T. J. (1995) Relationship of multidrug resistance to rhodamine-123 selectivity between carcinoma and normal epithelial cells: taxol and vinblastine modulate drug efflux. *Cancer Res.* **55**, 1633–1638.

Busciglio J., Lorenzo A., Yeh J. and Yanker B. A. (1995) β-Amyloid fibrils induce tau phosphorylation and loss of microtubule binding. *Neuron* **14**, 879–888.

Cavaletti G., Cavalletti E., Oggioni N., Sottani C., Minoia C., D'Incalci M., Zucchetti M., Marmiroli P. and Tredici G. (2000) Distribution of paclitaxel within the nervous system of the rat after repeated intravenous administration. *Neurotoxicology* **21**, 389–393.

Dhavan R., Tsai L. H. and Tsai L. H. (2001) A decade of cdk5. *Nat. Rev. Mol. Cell Biol.* **2**, 749–759.

Ding A. H., Porteu F., Sanchez E. and Nathan C. F. (1990) Shared actions of endotoxin and taxol on TNF receptors and release. *Science* **248**, 370–372.

Evans D. B., Rank K. B., Bhattacharya K., Thomsen D. R., Gurney M. E. and Sharma S. K. (2000) Tau phosphorylation at serine 396 and serine 404 by human recombinant tau protein kinase II inhibits tau's ability to promote microtubule assembly. *J. Biol. Chem.* **275**, 24977–24983.

Figueroa-Masot X. A., Hetman M., Higgins M. J., Kokot N. and Xia Z. (2001) Taxol induces apoptosis in cortical neurons by a mechanism independent of Bcl-2 phosphorylation. *J. Neurosci.* **21**, 4657–4667.

Goedert M. (1997) The neurofibrillary pathology of Alzheimer's disease. *Neuroscientist* **3**, 131–141.

Goedert M., Crowther R. A. and Spillantini M. G. (1998) Tau mutations cause frontotemporal dementias. *Neuron* **21**, 955–958.

He T. C., Zhou S., da Costa L. T., Yu J., Kinzler K. W. and Vogelstein B. (1998) A simplified system for generating recombinant adenoviruses. *Proc. Natl Acad. Sci. USA* **95**, 2509–2514.

Heimans J. J., Vermorken J. B., Wolbers J. G., Eeltink C. M., Meijer O. W., Taphoorn M. J. and Beijnen J. H. (1994) Paclitaxel (taxol) concentrations in brain tumor tissue. *Ann. Oncol.* **5**, 951–953.

Huang Y. and Wang K. K. (2001) The calpain family and human disease. *Trends Mol. Med.* **7**, 355–362.

Ino H., Ishizuka T., Chiba T. and Tatibana M. (1994) Expression of CDK5 (PSSALRE kinase), a neural cdc2-related protein kinase, in the mature and developing mouse central and peripheral nervous systems. *Brain Res.* **661**, 196–206.

Jordan M. A., Toso R. J., Thrower D. and Wilson L. (1993) Mechanism of mitotic block and inhibition of cell proliferation by taxol at low concentrations. *Proc. Natl Acad. Sci. USA* **90**, 9552–9556.

Kusakawa G., Saito T., Onuki R., Ishiguro K., Kishimoto T. and Hisanaga S. (2000) Calpain-dependent proteolytic cleavage of the p35 cyclin-dependent kinase 5 activator to p25. *J. Biol. Chem.* **275**, 17166–17172.

Lee V. M., Daughenbaugh R. and Trojanowski J. Q. (1994) Microtubule stabilizing drugs for the treatment of Alzheimer's disease. *Neurobiol. Aging* **15**, S87–S89.

Lee V. M., Goedert M. and Trojanowski J. Q. (2001) Neurodegenerative tauopathies. *Annu. Rev. Neurosci.* **24**, 1121–1159.

Lee K. Y., Clark A. W., Rosales J. L., Chapman K., Fung T. and Johnston R. N. (1999) Elevated neuronal Cdc2-like kinase activity in the Alzheimer disease brain. *Neurosci. Res.* **34**, 21–29.

Lee M. S., Kwon Y. T., Li M., Peng J., Friedlander R. M. and Tsai L. H. (2000) Neurotoxicity induces cleavage of p35 to p25 by calpain. *Nature* **405**, 360–364.

Liu Y., Ali S. M., Boge T. C., Georg G. I., Victory S., Zygmunt J., Marquez R. T. and Himes R. H. (2002) A systematic SAR study of C10 modified paclitaxel analogues using a combinatorial approach. *Comb. Chem. High Throughput Screen* **5**, 39–48.

Maccioni R. B., Otth C., Concha I. I. and Munoz J. P. (2001) The protein kinase Cdk5. Structural aspects, roles in neurogenesis and involvement in Alzheimer's pathology. *Eur. J. Biochem.* **268**, 1518–1527.

Manthey C. L., Qureshi N., Stutz P. L. and Vogel S. N. (1993) Lipopolysaccharide antagonists block taxol-induced signaling in murine macrophages. *J. Exp. Med.* **178**, 695–702.

Michaelis M. L., Walsh J. L., Pal R., Hurlbert M., Hoel G., Bland K., Foye J. and Kwong W. H. (1994) Immunologic localization and kinetic characterization of a Na^+/Ca^{2+} exchanger in neuronal and non-neuronal cells. *Brain Res.* **661**, 104–116.

Michaelis M. L., Ranciat N., Chen T., Bechtel M. R. R., Hepperle M., Liu Y. and Georg G. (1998) Protection against β-amyloid toxicity in primary neurons by paclitaxel (taxol). *J. Neurochem.* **70**, 1623–1627.

Michaelis M. L., Chen Y., Hill S., Reiff E., Georg G., Kice A. and Audus K. (2002) Amyloid peptide toxicity and microtubule-stabilizing drugs. *J. Mol. Neurosci.* **19**, 101–105.

Nakagawa T. and Yuan J. (2000) Cross-talk between two cysteine protease families. Activation of caspase-12 by calpain in apoptosis. *J. Cell Biol.* **150**, 887–894.

Nath R., Davis M., Probert A. W., Kupina N. C., Ren X., Schielke G. P. and Wang K. K. (2000) Processing of cdk5 activator p35 to its truncated form (p25) by calpain in acutely injured neuronal cells. *Biochem. Biophys. Res. Commun.* **274**, 16–21.

Nguyen M. D., Lariviere R. C. and Julien J. P. (2001) Deregulation of Cdk5 in a mouse model of ALS: toxicity alleviated by perikaryal neurofilament inclusions. *Neuron* **30**, 135–147.

Niethammer M., Smith D. S., Ayala R., Peng J., Ko J., Lee M. S., Morabito M. and Tsai L. H. (2000) NUDEL is a novel Cdk5 substrate that associates with LIS1 and cytoplasmic dynein. *Neuron* **28**, 697–711.

Nikolic M. and Tsai L. H. (2000) Activity and regulation of p35/Cdk5 kinase complex. *Meth Enzymol.* **325**, 200–213.

Patrick G. N., Zhou P., Kwon Y. T., Howley P. M. and Tsai L. H. (1998) p35, the neuronal-specific activator of cyclin-dependent kinase 5 (Cdk5) is degraded by the ubiquitin-proteasome pathway. *J. Biol. Chem.* **273**, 24057–24064.

Patrick G. N., Zukerberg L., de Nikolic M., La M. S., Dikkes P. and Tsai L. H. (1999) Conversion of p35 to p25 deregulates Cdk5 activity and promotes neurodegeneration. *Nature* **402**, 615–622.

Patrick G. N., Zukerberg L., de Nikolic M., La M. S., Dikkes P. and Tsai L. H. (2001) reply: p25 protein in neurodegeneration. *Nature* **411**, 764–765.

Patzke H. and Tsai L. H. (2002a) Calpain-mediated cleavage of the cyclin-dependent kinase 5 activator p39 to p29. *J. Biol. Chem.* **277**, 8054–8060.

Patzke H. and Tsai L. H. (2002b) Cdk5 sinks into ALS. *Trends Neurosci.* **25**, 8–10.

Rapoport M., Dawson H. N., Lester I. B., Vitek M. P. and Ferreira A. (2002) Tau is essential to β-amyloid-induced neurotoxicity. *Proc. Natl Acad. Sci. USA* **99**, 6364–6369.

Scheuner D., Eckman C., Jensen M., Song X., Citron M., Suzuki N., Bird T. D., Hardy J., Hutton M., Kukull W., Larson E., Levy-Lahad E., Viitanen M., Peskind E., Poorkaj P., Schellenberg G., Tanzi R., Wasco W., Lannfelt L., Selkoe D. and Younkin S. (1996) Secreted amyloid beta-protein similar to that in the senile plaques of Alzheimer's disease is increased *in vivo* by the presenilin 1 and 2 and APP mutations linked to familial Alzheimer's disease. *Nat. Med.* **2**, 864–870.

Selkoe D. J. (2001a) Alzheimer's disease: genes, proteins, and therapy. *Physiol. Rev.* **81**, 741–766.

Selkoe D. J. (2001b) Clearing the brain's amyloid cobwebs. *Neuron* **32**, 177–180.

Siman R., Flood D. G., Thinakaran G. and Neumar R. W. (2001) Endoplasmic reticulum stress-induced cysteine protease activation in cortical neurons: effect of an Alzheimer's disease-linked presenilin-1 knock-in mutation. *J. Biol. Chem.* **276**, 44736–44743.

Sobue K., Agarwal-Mawal A., Li W., Sun W., Miura Y. and Paudel H. K. (2000) Interaction of neuronal Cdc2-like protein kinase with microtubule-associated protein tau. *J. Biol. Chem.* **275**, 16673–16680.

Spillantini M. G., Murrell J. R., Goedert M., Farlow M. R., Klug A. and Ghetti B. (1998) Mutation in the tau gene in familial multiple system tauopathy with presenile dementia. *Proc. Natl Acad. Sci. USA* **95**, 7737–7741.

Taniguchi S., Fujita Y., Hayashi S., Kakita A., Takahashi H., Murayama S., Saido T. C., Hisanaga S., Iwatsubo T. and Hasegawa M. (2001) Calpain-mediated degradation of p35 to p25 in postmortem human and rat brains. *FEBS Lett.* **489**, 46–50.

Teraski T. and Tsuji A. (1995) Controlling transport and metabolism, in *Peptide Based Drug Design* (Taylor M. D. and Amidon G. L., eds), pp. 297–316. Amer. Chem. Soc., Washington, DC.

Thiel V. E. and Audus K. L. (2001) Nitric oxide and blood–brain barrier integrity. *Antioxid. Redox Signal.* **3**, 273–278.

Tsai L. H., Delalle I., Caviness V. S. Jr, Chae T. and Harlow E. (1994) p35 is a neural-specific regulatory subunit of cyclin-dependent kinase 5. *Nature* **371**, 419–423.

Wang K. K. (2000) Calpain and caspase: can you tell the difference? *Trends Neurosci.* **23**, 20–26.

Wang T. H., Wang H. S., Ichijo H., Giannakakou P., Foster J. S., Fojo T. and Wimalasena J. (1998) Microtubule-interfering agents activate c-Jun N-terminal kinase/stress-activated protein kinase through both Ras and apoptosis signal-regulating kinase pathways. *J. Biol. Chem.* **273**, 4928–4936.

Xie H. and Johnson G. V. (1997) Ceramide selectively decreases tau levels in differentiated PC12 cells through modulation of calpain I. *J. Neurochem.* **69**, 1020–1030.

Yoneda T., Imaizumi K., Oono K., Yui D., Gomi F., Katayama T. and Tohyama M. (2001) Activation of caspase-12, an endoplastic reticulum (ER) resident caspase, through tumor necrosis factor receptor-associated factor 2-dependent mechanism in response to the ER stress. *J. Biol. Chem.* **276**, 13935–13940.

Yoo B. C. and Lubec G. (2001) p25 protein in neurodegeneration. *Nature* **411**, 763–764.

Zukerberg L. R., Patrick G. N., Nikolic M., Humbert S., Wu C. L., Lanier L. M., Gertler F. B., Vidal M., Van Etten R. A. and Tsai L. H. (2000) Cables links Cdk5 and c-Abl and facilitates Cdk5 tyrosine phosphorylation, kinase upregulation, and neurite outgrowth. *Neuron* **26**, 633–646.

Journal of Molecular Neuroscience

ISSN0895-8696/03/20:339–343/$25.00

ALZHEIMER'S THERAPEUTICS: Neuroprotection

Overcoming the Blood–Brain Barrier to Taxane Delivery for Neurodegenerative Diseases and Brain Tumors

Antonie Rice,[1] Mary L. Michaelis,*[,2] Gunda Georg,[3] Yanbin Liu,[3] Brandon Turunen,[3] and Kenneth L. Audus[1]

[1]Department of Pharmaceutical Chemistry, University of Kansas, 226 Simons, 2095 Constant Avenue, Lawrence, KS 66047; and [2]Department of Pharmacology and Toxicology and [3]Medicinal Chemistry, University of Kansas, 1251 Wescoe Hall Drive, Lawrence, KS 66045

Received October 15, 2002; Accepted March 24, 2003

Abstract

The blood–brain barrier (BBB) effectively prevents microtubule (MT)-stabilizing drugs from readily entering the central nervous system (CNS). A major limiting factor for microtubule-stabilizing drug permeation across the BBB is the active efflux back into the circulation by the overexpression of the multidrug-resistant gene product 1 (MDR1) or P-glycoprotein (P-gp). This study has focused on strategies to overcome P-gp-mediated efflux of Taxol analogs, MT-stabilizing agents that could be used to treat brain tumors and, potentially, neurodegenerative diseases such as Alzheimer's disease. However, taxol is a strong P-gp substrate that limits its distribution across the BBB and therapeutic potential in the CNS. We have found that addition of a succinate group to the C-10 position of paclitaxel (Taxol) results in an agent, Tx-67, with reduced interactions with P-gp and enhanced permeation across the BBB in both in vitro and *in situ* models. Our studies demonstrate the feasibility of making small chemical modifications to Taxol to generate analogs with reduced affinity for the P-gp but retention of MT-stabilizing properties, i.e., a taxane that may reach and treat therapeutic targets in the CNS.

Index Entries: Blood–brain barrier; CNS drug permeation; microtubule-stabilizing drugs; Taxol; brain microcapillary endothelial cells; neurofibrillary pathology.

Introduction

The delivery of therapeutic agents into the brain continues to be a challenge for the pharmaceutical industry. Because of the inadequate delivery of these agents to the desired site of action in the brain, many neurological disorders (i.e., brain tumors, Alzheimer's disease, and other brain disorders) have poor responses to drug treatment (Pardridge, 2002). We have previously shown in neuronal cell cultures that the microtubule (MT)-stabilizing drug Taxol protects neurons against amyloid peptide (Aβ) toxicity (Michaelis et al., 1998, 2002). The potential for testing protective effects in vivo is severely limited by the failure of Taxol and several of its derivatives to enter the brain. Consequently, we have synthesized a large array of MT-stabilizing drugs related to Taxol and tested them for potential to penetrate into the brain. In this paper we discuss the strategies we have tested and the results obtained regarding brain permeability of one promising taxane.

The blood–brain barrier (BBB) regulates the influx and efflux of a wide variety of substances and remains the major obstacle in the delivery of drugs into the central nervous system (CNS). The most common mechanism for drug distribution across the

*Author to whom all correspondence and reprint requests should be addressed. E-mail: mlm@ku.edu

BBB is by simple passive diffusion; however, once a drug enters the endothelial lining of the BBB by this mechanism, it may either undergo passive diffusion or active transport back out of the cells into the circulation. First identified in tumors, the active efflux transport mechanisms are implicated as major factors in limiting the effective delivery of a number of drugs and drug classes across the BBB (Schinkel, 1999; Taylor, 2002). The transporters responsible for the active efflux of drugs at the BBB include the multidrug-resistant gene product 1 (MDR1) or P-glycoprotein (P-gp), multidrug resistance-associated proteins, and the breast cancer resistance protein. The major efflux pump at the BBB is MDR1 or P-gp (Schinkel, 1999; Taylor, 2002).

P-glycoprotein is a member of the ATP-binding cassette (ABC) family of transport proteins (Gottesman et al., 1996). This transporter is located on the blood side of the capillary endothelial cell and is involved in the efflux of a wide range of substrates that include antineoplastic agents (e.g., vincristine, vinblastine, and Taxol), antiviral compounds (e.g., saquinavir, ritonavir, indinavir), opiates, and other therapeutic agents. Various strategies have been devised to circumvent the BBB to increase drug delivery to the CNS. These strategies involve attempts to manipulate either the chemical properties of the agent, opening the BBB by increasing capillary endothelial permeability, or enhancing the driving force for transport by increasing the plasma concentration of a drug (i.e., high-dose chemotherapy, intra-arterial injection) (Taylor, 2002; Siegal and Zylber-Katz, 2002).

The strategy we chose to overcome the BBB efflux mechanisms was to focus on the use of combinatorial chemistry to manipulate chemical structure in order to reduce affinity for P-gp. This type of approach has been used successfully, for example, to generate molecular diversity in chemical structures for the development of new antibacterial agents in order to overcome bacterial drug resistance (Desnottes, 1996). The starting point for our work was to generate and screen newly synthesized analogs of the anticancer agent, paclitaxel or Taxol, for taxanes that have reduced P-gp affinity relative to the parent drug. Taxol, one of the leading anticancer drugs currently on the market for the treatment of ovarian and breast cancer, is very effective in treating tumors but, unfortunately, is also a substrate for the P-gp efflux pump. Because of interactions with P-gp at the BBB, it is almost impossible to infuse Taxol vascularly to treat brain tumors (Cahan et al., 1994; Brouty-Boye et al., 1995; Lovich et al., 2001; Fellner et al., 2002). Therefore, second-generation taxanes that retain appropriate pharmacological activity and have reduced interactions with P-gp were generated with the primary objective of improving distribution across the BBB. To characterize these new taxanes we have employed a combination of in vitro and *in situ* models of the BBB. The goals of the experiments described herein were to (1) determine which newly synthesized taxanes have reduced P-gp interactions and improved permeability properties relative to Taxol, using an in vitro model comprised of P-gp-expressing primary cultures of bovine brain microvessel endothelial cells (BBMECs); and (2) determine which newly synthesized taxanes have improved permeability properties relative to Taxol at the BBB, using an *in situ* rat brain perfusion model. Taxol and the taxanes that were employed in the permeability assays here have been shown previously to retain appropriate pharmacological properties with respect to protecting neurons against Aβ-induced toxicity (Michaelis et al., 1998, 2002).

Materials and Methods

BBMECs were isolated from the gray matter of cerebral cortices by enzymatic digestion and subsequent centrifugation, and seeded into primary culture as described (Audus and Borchardt, 1987; Audus et al., 1996). Uptake and transport studies were performed in pH 7.4 standard buffer solutions, consisting of either Hank's balanced salt solution or phosphate-buffered saline (PBS) supplemented with 0.63 m*M* $CaCl_2$, 0.74 m*M* $MgSO_4$, 5.3 m*M* glucose, and 0.1 m*M* ascorbic acid (PBSA). [^{3}H]Taxol (sp. act. 10.5 Ci/mmol) was obtained from Moravek Radiochemicals. Dr. Gunda Georg (Medicinal Chemistry Department, University of Kansas), supplied the Taxol and taxane analogs. Rhodamine 123 (Rho 123) and cyclosporin A (CsA) were obtained from Sigma.

Rho 123 Accumulation in the Presence of Taxanes

BBMECs were grown in 12-well plates to form confluent monolayers and used as described to assay for P-gp as detailed elsewhere (Rose et al., 1998). Briefly, the fluorescent marker Rho 123 was dissolved in PBSA buffer to give a stock concentration of 100 μ*M*. The uptake assay was performed in 1 mL of fresh PBSA. An aliquot of Taxol or one of its analogs

was added to each well to give a final concentration of 25 μ*M*. As a positive control, the P-gp inhibitor CsA (5–10 μ*M*) was used. The negative control was rhodamine (5–10 μ*M*) alone. The cells were preincubated at 37°C with Taxol or an analog for ~45 min. After this preincubation period, Rho 123 was added to the cells. After a 45-min incubation, the cells were washed in cold PBS and lysed in a NaOH/Triton X-100 solution. The cell lysates were assayed using a fluorescence spectrophotometer. Rhodimine 123 was measured at excitation/emission wavelengths of 500 nm/535 nm and quantified against a standard curve of Rho 123 in the appropriate lysing solution. The protein content was determined using the bicinchoninic acid (BCA) protein assay reagent kit and the results were expressed as total fluorescence accumulation per milligram of cell protein.

Transport of Taxanes Across BBMEC Monolayers

The BBMECs were grown on 0.4-μm pore polycarbonate membranes essentially as described (Audus and Borchardt 1987; Audus et al. (1996). When they reached confluency, the cells were transferred to side-by-side diffusion chambers to characterize the transport of a small number of promising tritium-labeled compounds by assessing their permeability relative to that of the paracellular marker [^{14}C] sucrose as an index of monolayer confluency. Bidirectional transport was assessed for each of the radiolabeled compounds to determine if polarized transport was observed. All of the studies were performed in 3 mL of stirred PBSA in each donor and receiver chamber at 37°C. The cells were allowed to equilibrate in PBSA for 30 min prior to the experiment. At each time point, 100 μL of sample was taken from the receiver compartment and replaced immediately with an equal volume of PBSA. Apparent permeability coefficients (P_{app}) were calculated according to the following equation, $P_{app} = (V/AC_o) * (dC/dt)$ where V = volume of the receiver chamber (3.0 cm^3), A = area of the filter (0.636 cm^2), C_o = initial donor concentration, and (dC/dt) = flux of the test agent.

In Situ *Rat Brain Perfusion of Taxanes*

The *in situ* rat brain perfusion technique described by Smith (1996), was employed to determine the BBB permeability of Taxol and the taxane analog Tx-67. Adult male Sprague-Dawley rats (350–400 g) were anesthetized with a mixture containing: 1.5 mL/kg of solution consisting of 37.5 mg/mL ketamine, 1.9 mg/mL xylazine, and 0.37 mg/mL acepromazine. The rat brain was then directly perfused through the left carotid artery with a buffered physiologic saline containing a tracer (sucrose) as a vascular marker and the sample ([^{3}H] Taxol or [^{14}C] Tx-67) for time periods of 30, 60, or 120 s. The perfusion solution was changed to tracer-free fluid for 30 s to clear the labeled compound from the cerebral vessels. After the perfusion, the rat was decapitated and the brain removed for the sampling of various regions. The brain tissue was digested in Solvable for 24 h and the radioactivity quantified via liquid scintillation spectrometry. The capillary permeability-surface area product (PA) (mL/s/g) was calculated for both Taxol and Tx-67 by the following equation, $PA = -F \text{ Ln } [1-C^*br\,(T)/F\,T\,C^*pf]$ where F is the regional cerebral blood flow (mL/s/g), C^*br represents the concentration of tracer in the brain parenchyma (dpm/g), C^*pf is the concentration in the perfusion fluid (dpm/mL), and T is the total perfusion time.

Results

Rhodamine 123 accumulation was assessed in the presence of Taxol and the new analogs of Taxol. Although it is an indirect assay, our studies revealed that some of the synthetic taxanes appeared to have reduced interactions with P-gp (i.e., no increase in Rho 123 accumulation in the presence of the analogs). Taxol, a known substrate for P-gp, increased rhodamine uptake by 2-to 2.5-fold in the BBMECs. Rhodamine uptake in the presence of Taxol was very similar to that observed in the presence of the positive control, CsA (5 μ*M*), a known P-gp inhibitor. Accordingly, from the Rho 123 screening of numerous taxanes in multiwell dish formats, we obtained a rather quick analysis of which taxanes were poor substrate for efflux by P-gp. One of the taxanes that had no apparent interactions with P-gp, that is, no effect on Rho 123 uptake by BBMECs, was designated Tx-67, a compound in which a succinate group was added at the C-10 position of Taxol.

We next assessed the actual permeability properties of Tx-67 relative to Taxol. Given that the BBMECs have an apical (a) and a basolateral (b) surface when grown on polycarbonate membranes, our permeation studies included an assessment of whether the permeation was polarized or asymmetric in nature. We used radiolabeled Taxol and Tx-67 for these experiments to provide sensitivity in the nanomolar concentration range. The apparent permeability coefficient for Taxol was greater in the *b* to *a* direction (i.e., *b*—*a* > *a*—*b*). We also observed that the

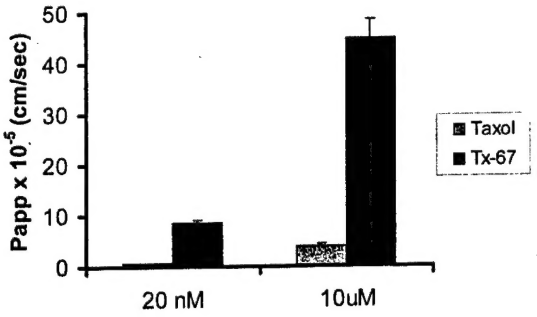

Fig. 1. Concentration dependence of apparent permeability coefficients (P_{app}) for Taxol and Tx-67 permeation across primary cultures of BBMEC monolayers at 37°C. The data summarized are the P_{app} for taxane permeation from the apical (blood) to basolateral (brain) side of the monolayers. The data points are means ± S.D. for at least four different monolayers.

Table 1
Apparent Permeability Coefficients for [^{14}C]Tx-67 and [^{3}H]Taxol in *In Situ* Rat Brain Perfusion

	P_{app} x 107 cm/s		
Compound	30 s	60 s	120 s
[^{14}C]Tx-67	8.47	13.71	10.75
[^{3}H]Taxol	0.845	1.700	1.574

Time points were for 30, 60, and 120 s (each time point was determined in duplicate experiments).

analog Tx-67 had enhanced permeation compared to that of Taxol. The apparent permeability coefficient of Tx-67 at any concentration (low or high) was substantially greater than the P_{app} for Taxol at the highest concentration used (25 μ*M*). Moreover, the permeation of Tx-67 was asymmetric but greater in the a to b direction, which suggests greater blood to brain permeation for the new taxane. Fig. 1 shows typical results for Taxol and Tx-67 permeability at 20 n*M*, a concentration at which the BBMEC P-gp is not saturated, and at 10 μ*M*, a concentration at which the transporter is presumed to be saturated and thus the permeability of the monolayers to both agents significantly increased. It is important to note that BBMEC monolayer permeability to radiolabeled sucrose (i.e., a marker for integrity and background monolayer "leakage") was not altered by exposure to either Taxol or Tx-67 under the conditions of these experiments.

In the *in situ* perfusion experiments with [^{14}C]Tx-67 and [^{3}H]Taxol, we observed a substantially greater apparent permeability coefficient for Tx-67 relative to Taxol. It appears that Taxol is not retained in the rat brain tissue, as only minimal amounts (2.5% or less of total control) were detectable in the brain at 120 s. Approximately 6–8% of the total Tx-67 was detectable after 60 s of perfusion. Table 1 lists the P_{app} determined for Tx-67 and Taxol at each perfusion time.

Discussion

The initial Rho 123 screening of newly synthesized taxanes showed that some structural modifications to Taxol generated through combinatorial chemistry approaches lead to compounds that appear to be less avid substrates for P-gp than the parent Taxol. Clearly, Taxol competes with Rho 123 for P-gp, resulting in increased fluorescence using this screening technique. On the other hand, Tx-67 appeared to interact with P-gp to a significantly lesser degree in the same assay. Despite the addition of the succinyl group, Tx-67 retained its MT-stabilizing properties and its effectiveness in protecting neurons against Aβ-induced toxicity, as reported earlier (Michaelis et al., 2002). These findings are consistent with studies in other laboratories that show second-generation taxanes have reduced interactions with P-gp and yet still exhibit potent anticancer activity (Ojima et al., 1996; Ojima and Slater, 1997).

We also determined that the transport of Taxol across BBMEC monolayers was asymmetric and supports previous data that the P-gp is localized on the apical side of the brain (Cordon-Cardo et al., 1989; Tsuji et al., 1992). However, the new taxane, Tx-67, although asymmetric in permeation across the monolayers, showed a much higher permeability, favoring what would be blood to brain distribution in this model. The *in situ* rat brain perfusion data correlated well with our in vitro permeability data, showing that Tx-67 permeation across the BBB was in fact substantially greater than the permeation of Taxol into rat brains. Our Taxol data were comparable to perfusion data for other anticancer drugs such as vincristine and vinblastine (Greig et al., 1990).

We have demonstrated that the use of combinatorial chemistry led to synthesis of new taxanes with reduced interactions with P-gp. We have also been able to demonstrate that one of the newly synthesized analogs, Tx-67, appears to cross the BBB both in vitro and *in situ* more readily than the parent drug. The Tx-67 permeation studies support our hypothesis that chemical modification of Taxol does enhance its permeability into the brain. In addition, the work

is consistent with literature observations in which small changes in chemical structures can alter interactions with P-gp at the BBB and thereby influence the distribution of the agents into the CNS (Mann et al., 1997). The most significant aspect of these results is that we now have an agent with MT-stabilizing activity and strong neuroprotective actions against Aβ in primary neuronal cultures that can be tested in vivo. Studies are being undertaken to characterize the pharmacokinetic and pharmacodynamic properties of Tx-67 in mice. This is being done in anticipation of testing its therapeutic potential in animal models of both neurodegenerative diseases and brain tumors.

Acknowledgments

This work was supported by the Institute for the Study of Aging (New York) and an NIH grant (NCI 1 RO1 CA82801).

References

Audus K. L. and Borchardt R. T. (1987) Bovine brain microvessel endothelial cell monolayers as a model system for the blood-brain barrier. *Ann. NY Acad. Sci.* **507,** 9–18.

Audus K. L., Ng L., Wang W., and Borchardt R. T. (1996) Brain microvessel endothelial cell culture systems. *Pharm. Biotechnol.* **8,** 239–258.

Brouty-Boye D., Kolonias D., Wu C. J., Savaraj N., and Lampidis T. J. (1995) Relationship of multidrug resistance to rhodamine-123 selectivity between carcinoma and normal epithelial cells: taxol and vinblastine modulate drug efflux. *Cancer Res.* **55,** 1633–1638.

Cahan M. A., Walter K. A., Colvin O. M., and Brem H. (1994) Cytotoxicity of taxol in vitro against human and rat malignant brain tumors. *Cancer Chemother. Pharmacol.* **33,** 441–444.

Cordon-Cardo C., O'Brien J. P., Casals D., Rittman-Grauer L., Biedler J. L., Melamed M. R., and Bertino J. R. (1989) Multidrug-resistance gene (P-glycoprotein) is expressed by endothelial cells at blood-brain barrier sites. *Proc. Natl. Acad. Sci. USA* **86,** 695–698.

Desnottes J. F. (1996) New targets and strategies for the development of antibacterial agents. *Trends Biotechnol.* **14,** 134–140.

Fellner S., Bauer B., Miller D.S., Schaffrik M., Franhanel M., Spruss T., et al. (2002) Transport of paclitaxel (Taxol) across the blood-brain barrier in vitro and in vivo. *J. Clin. Invest.* **110,** 1309–1318.

Gottesman M. M., Pastan I., and Ambudkar S. V. (1996) P-glycoprotein and multidrug resistance. *Curr. Opin. Genet. Dev.* **6,** 610–617.

Greig N. H., Soncrant T. T., Shetty H. U., Momma S., Smith Q. R., and Rapoport S. I. (1990) Brain uptake and anticancer activities of vincristine and vinblastine are restricted by their low cerebrovascular permeability and binding to plasma constituents in rat. *Cancer Chemother. Pharmacol.* **26,** 263–268.

Lovich M. A., Creel C., Hong K., Hwang C. W., and Edelman E. R. (2001) Carrier proteins determine local pharmacokinetics and arterial distribution of paclitaxel. *J. Pharm. Sci.* **90,** 1324–1335.

Mann H., Ladenheim B., Hirata H., Moran T. H., and Cadet J. L. (1997) Differential toxic effects of methamphetamine (METH) and methylenedioxymethamphetamine (MDMA) in multidrug resistant (mdr1a) knockout mice. *Brain Res.* **769,** 340–346.

Michaelis M. L., Chen Y., Hill S., Reiff E., Georg G., Rice A., and Audus K. L. (2002) Amyloid peptide toxicity and microtubule-stabilizing drugs. *J. Mol. Neurosci.* **19,** 101–105.

Michaelis M. L., Ranciat N., Chen Y., Bechtel M., Ragan R., Hepperle M., et al. (1998) Protection against β-amyloid toxicity in primary neurons by paclitaxel (Taxol). *J. Neurochem.* **70,** 1623–1627.

Ojima I. and Slater J. C. (1997) Synthesis of novel 3'-trifluoromethyl taxoids through effective kinetic resolution of racemic 4-CF3-beta-lactams with baccatins. *Chirality* **9,** 487–494.

Ojima I., Slater J. C., Michaud E., Kuduk S. D., Bounaud P. Y., Vrignaud P., et al. (1996) Syntheses and structure-activity relationships of the second-generation antitumor taxoids: exceptional activity against drug-resistant cancer cells. *J. Med. Chem.* **39,** 3889–3896.

Pardridge W. M. (2002) Targeting neurotherapeutic agents through the blood-brain barrier. *Arch. Neurol.* **59,** 35–40.

Rose J. M., Peckham S. L., Scism J. L., and Audus K. L. (1998) Evaluation of the role of P-glycoprotein in ivermectin uptake by primary cultures of bovine brain microvessel endothelial cells. *Neurochem. Res.* **23,** 203–209.

Schinkel A. H. (1999) P-Glycoprotein, a gatekeeper in the blood-brain barrier. *Adv. Drug Deliv. Rev.* **36,** 179–194.

Siegal T. and Zylber-Katz E. (2002) Strategies for increasing drug delivery to the brain: focus on brain lymphoma. *Clin. Pharmacokinet.* **41,** 171–186.

Smith Q. (1996) Brain perfusion systems for studies of drug uptake and metabolism in the central nervous system. *Pharm. Biotechnol.* **8,** 285–307.

Taylor E. M. (2002) The impact of efflux transporters in the brain on the development of drugs for CNS disorders. *Clin. Pharmacokinet.* **41,** 81–92.

Tsuji A., Terasaki T., Takabatake Y., Tenda Y., Tamai I., Yamashima T., et al. (1992) P-glycoprotein as the drug efflux pump in primary cultured bovine brain capillary endothelial cells. *Life Sci.* **51,** 1427–1437.